

TR 3.1
MIMO CHANNEL MODELS

16TH SEPTEMBER 2011

Editor: Tero Jokela
University of Turku, Finland



TR 3.1

List of contributors

BBC

CNES

Digita

Elektrobit

Nokia

Tampere University of Technology

Turku University of Applied Sciences

University of Turku (editor)

Table of Contents

1	Introduction	5
2	Measurement signal definition	5
2.1	OFDM frame structure	6
2.2	Reference signals.....	6
2.3	TPS pilots	7
2.4	Data carriers.....	7
3	Measurement campaign.....	8
3.1	Locations	8
3.2	Block Diagram Setup.....	9
3.3	Application Antennas	10
3.4	Transmitter	10
3.5	Modulator	11
3.6	Coverage prediction.....	12
3.7	Portable Receiver (for data capture).....	12
3.8	Campaign Schedule	13
3.9	Channel models	14
4	Defined Channel Models (DVB-NGH Channel Models).....	14
4.1	Single-Input-Single-Output (SISO) Channel models	14
4.1.1	Stationary reception.....	14
4.1.2	Portable reception	15
4.1.3	Mobile Reception	15
4.2	Multiple-Input-Multiple-Output (MIMO) Channel models	17
4.2.1	General approach.....	17
4.2.2	Outdoor portable model.....	17
4.2.3	Indoor portable model	20
4.2.4	Additional antenna rotation and asymmetry terms	22
4.2.5	Simulation practicalities	23
4.2.6	Generating fixed channel realizations (0Hz Doppler snapshots).....	23
4.2.7	Mobile vehicular outdoor model	23
4.2.8	4 x 2 model (& 2-tower SFN).....	23
4.3	Satellite and hybrid channel models.....	24
4.3.1	Hybrid channel software.....	24
4.3.1.1	SISO hybrid propagation channel.....	24
4.3.1.2	MIMO extension.....	29
4.3.2	LMS SISO & MIMO physical-statistical model for Tree Shadowed environments	30
4.3.2.1	SISO physical model	30
4.3.2.2	MIMO extension.....	33
4.3.2.3	Reference parameterization	35



TR 3.1

4.3.3	LMS SISO & MIMO empirical models	36
4.3.3.1	SISO empirical models.....	36
4.3.3.2	MIMO extension.....	44
4.4	SISO, MISO and SIMO systems	47
5	References	47

Abstract –MIMO (Multiple-In Multiple-Out) mechanisms allow for increased diversity or data rate as compared to a communications system with single transmitting and receiving antenna. Multiple antenna schemes are not currently widely utilized for broadcasting. Therefore, not many realistic channel models are available. As suitable MIMO schemes for broadcasting need to be studied for DVB-NGH system, common channel model are necessary. In this document, such channel models for cross-polar MIMO in terrestrial, satellite and hybrid scenarios are presented. In addition to the channel models, the measurement processes for generating them are described.

1 INTRODUCTION

In this report the MIMO (Multiple-Input Multiple-Output) channel models created for DVB-NGH system design are presented. The channel models are generated based on field measurements. This report consists of three main parts, definition of the signal used for the terrestrial measurements, the measurement campaign report and the resulting channel model descriptions.

The terrestrial measured signal is based the OFDM format of DVB-T. The first transmitter radiates DVB-T scattered pilots, continual pilots and TPS pilots exactly as defined in [1]. Since 2-transmitter MIMO channel measurement is required, modifications to the signal for the second transmitter are necessary. These are as follows: on every other OFDM symbol, the sign of the scattered pilots is reversed (i.e. the pilot is inverted) with respect to that defined in [1].

A high-power terrestrial 2-by-2 cross-polar MIMO channel sounding campaign was carried out in the city of Helsinki, Finland, as part of the DVB-NGH MIMO investigation. This was carried out in collaboration with BBC, Digita, Elektrobit, Nokia, Tampere University and Turku University of Applied Sciences (TUAS) which are involved with the Celtic ENGINES project.

The channel models that have been created on the basis of the measurements are presented in this document. The target is to give common definitions of channel models for all who will use them in simulations and laboratory measurements. A variety of models are included to cover a wide range of transmission and reception conditions. Transmission conditions addressed contain different numbers of transmission antennas and different types of transmitter configurations such as terrestrial, satellite and hybrid. Also specific channel definitions for testing receiver synchronization issues in SFN-conditions are included.

2 MEASUREMENT SIGNAL DEFINITION

The proposed signal is based the OFDM format of DVB-T. This signal is defined in [1] and features a 1-in-12 pilot structure intended for channel estimation. The first transmitter radiates DVB-T scattered pilots, continual pilots and TPS pilots exactly as defined in [1]. Since 2-transmitter MIMO channel measurement is required, modifications to the signal for the second transmitter are necessary. These are as follows: on every other OFDM symbol, the sign of the scattered pilots is reversed (i.e. the pilot is inverted) with respect to that defined in [1]. In addition, continual pilots which lie on carriers which at times coincide with an inverted pilot are permanently inverted to allow consistency when they are indeed coincident.

TPS data is arbitrary as it is not anticipated it will be used in the channel measurement applications.

The data cells are assigned fixed BPSK data obtained from the DVB-T reference sequence of [1] para. 4.5.2.

2.1 OFDM frame structure

OFDM frame structure shall be as reference [1] paragraph 4.4 with the following changes/exceptions:

2k mode only
8MHz channel only

2.2 Reference signals

Location of scattered pilots

Reference information, taken from the reference sequence of [1] para. 4.5.2, is transmitted in scattered pilot cells in every symbol. Scattered pilot cells are always transmitted at the "boosted" power level of 16/9 relative to data bearing carriers. Thus the corresponding modulation is given by:

$$\operatorname{Re}\{c_{m,l,k}\} = \frac{4}{3} \times 2 \left(\frac{1}{2} - w_k \right)$$

$$\operatorname{Im}\{c_{m,l,k}\} = 0$$

where m is the frame index, k is the frequency index of the carriers and l is the time index of the symbols.

For the symbol of index l (l ranging from 0 to 67), carriers for which index k belongs to the subset $k = K_{\min} + 3 \times (l \bmod 4) + 12p$ (p integer, $p \geq 0$, k in range $[K_{\min}; K_{\max}]$) are scattered pilots. The pilot insertion pattern is shown in figure 11 of [1] 4.5.3.

Location and modulation of continual pilots

In addition to the scattered pilots, 45 locations for continual pilots are defined in [1] para. 4.5.4 for 2k mode.

All continual pilots are modulated according to the reference sequence, see ref. [1] para. 4.5.2.

The continual pilots are transmitted at "boosted" power level.

Thus the corresponding modulation is given by, on transmitter 1 of 2:

$$\operatorname{Re}\{c_{m,l,k}\} = \frac{4}{3} \times 2 \left(\frac{1}{2} - w_k \right)$$

$$\operatorname{Im}\{c_{m,l,k}\} = 0$$

Modification to pilots on transmitter 2

Transmitter 2 has scattered pilots inverted every other OFDM symbol to allow for MIMO channel measurement. Continual pilots falling on scattered-pilot-bearing carriers are inverted compared to transmitter 1 if the coincident scattered pilot is inverted; continual pilots without this property are not inverted.

Scattered pilots on transmitter 2:

$$\operatorname{Re}\{c_{m,l,k}\} = \frac{4}{3} \times (-1)^l \times 2 \left(\frac{1}{2} - w_k \right) \quad (\text{symbol no. } l \text{ in the range } 0 \dots 67)$$

$$\operatorname{Im}\{c_{m,l,k}\} = 0$$

Continual pilots on transmitter 2:

$$\operatorname{Re}\{c_{m,l,k}\} = \frac{4}{3} \times (-1)^l \times 2 \left(\frac{1}{2} - w_k \right) \quad \text{if } k \bmod 3 = 0$$

$$\operatorname{Re}\{c_{m,l,k}\} = \frac{4}{3} \times 2 \left(\frac{1}{2} - w_k \right) \quad \text{otherwise}$$

$$\operatorname{Im}\{c_{m,l,k}\} = 0$$

Amplitudes of all reference information

Reference [1] para 4.5.5 shall apply.

2.3 TPS pilots

This is defined in accordance with [1] para. 4.6, 2k mode, but may have arbitrary information in s_0 - s_{67} .

2.4 Data carriers

Location and modulation of the data carriers

The set of data carriers associated with the l^{th} symbol of the m^{th} transmission frame has 1512 elements and is denoted here by $\{data\ carriers\}_{m,l}$. It is the complement of the set of reference and TPS carriers, and we shall index it with v in the range $(0 \dots 1511)$

Transmitter 1:

Data carriers depend only on the indices v and l and are given by

$$\operatorname{Re}\{c_{m,l,v}^{(1)}\} = 2 \left(\frac{1}{2} - d_{v,l} \right) \quad \text{for } v \in \{0 \dots 1511\} \text{ and } l \in \{0 \dots 67\}$$

$$\operatorname{Im}\{c_{m,l,v}\} = 0$$

with $d_{v,l}$, as specified in the following section.

Transmitter 2:

Data carriers depend on the indices v and l and are given by

$$\operatorname{Re}\{c_{m,l,v}^{(2)}\} = (-1)^l \times 2 \left(\frac{1}{2} - d_{v,l} \right) \quad \text{for } v \in \{0 \dots 1511\} \text{ and } l \in \{0 \dots 67\}$$

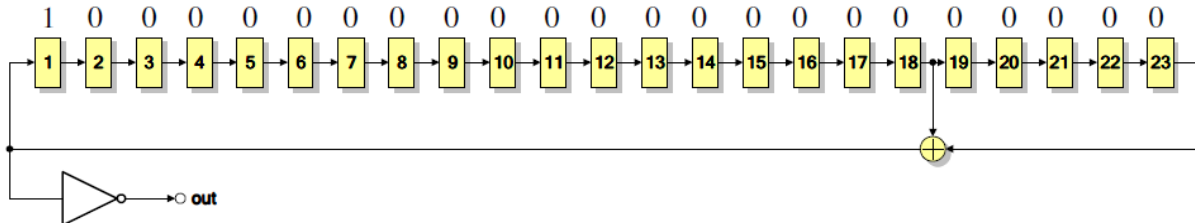
$$\operatorname{Im}\{c_{m,l,v}\} = 0$$

with $d_{v,l}$, as specified in the following section.

PRBS sequence of the data carriers

The data carriers are modulated according to a different PRBS sequence, $d_{v,l}$ corresponding to their respective data carrier index v and the frame index l . This PRBS sequence with its initialization sequence is shown in the diagram below.

Initialisation sequence



The PRBS is initialised so that the first output bit from the PRBS coincides with the first active carrier (data or signalling) of the first OFDM symbol in the frame, i.e. $l=0$. Subsequent bits from the sequence are mapped in order to the active carriers in the remaining symbols in the frame $l=1$ to $l=67$. However if the carrier is not a data carrier, the PRBS output is discarded. In this way, within the l^{th} symbol, 1705 bits are generated by the PRBS but only 1512 are used corresponding to v in the range $0 \dots 1511$.

So if the sequence is u_m with $m \in 0 \dots (1705 * 68) - 1$ then we can write (as pseudocode)

```
F=68;
P=1705;
for l=0:F-1
    v=0;
    for p=0:P-1
        if carrier==data_carrier
            d(v,l)=u(p+1*P);
            v=v+1;
        end
    end
end
end
```

The PRBS will be re-initialised at the start of every OFDM frame.

The polynomial for the PRBS generator for data carriers is $X^{23} + X^{18} + 1$, as specified by ITU-T recommendation O.151, clause 2.2.

3 MEASUREMENT CAMPAIGN

A high-power 2-by-2 cross-polar MIMO channel sounding campaign was carried out in the city of Helsinki, Finland, as part of the DVB-NGH MIMO investigation. This was carried out in collaboration with BBC, Digita, Elektrobit, Nokia, Tampere University and Turku University of Applied Sciences (TUAS) which are involved with the Celtic ENGINES project. Amphenol has kindly assist in the sounding by providing an application antenna. The channel sounding campaign was scheduled for 5 days starting from Monday the 28th of June 2010. The data collected from the measurement campaign will be processed to obtain a realistic 2-by-2 cross-polar MIMO channel model to be used in simulation for technical proposal evaluation.

3.1 Locations

The channel data was recorded in 4 different locations:

1. Digita office (indoor and outdoor)

2. Outdoor measurement at the Helsinki Olympic stadium car park (outdoor)
3. Tekes office (indoor and outdoor walkway)
4. High power non-line-of-sight outdoor (near Pasila Tower / Tekes office)

These locations are indicated in Figure 1 below along with the location of the transmitting tower.

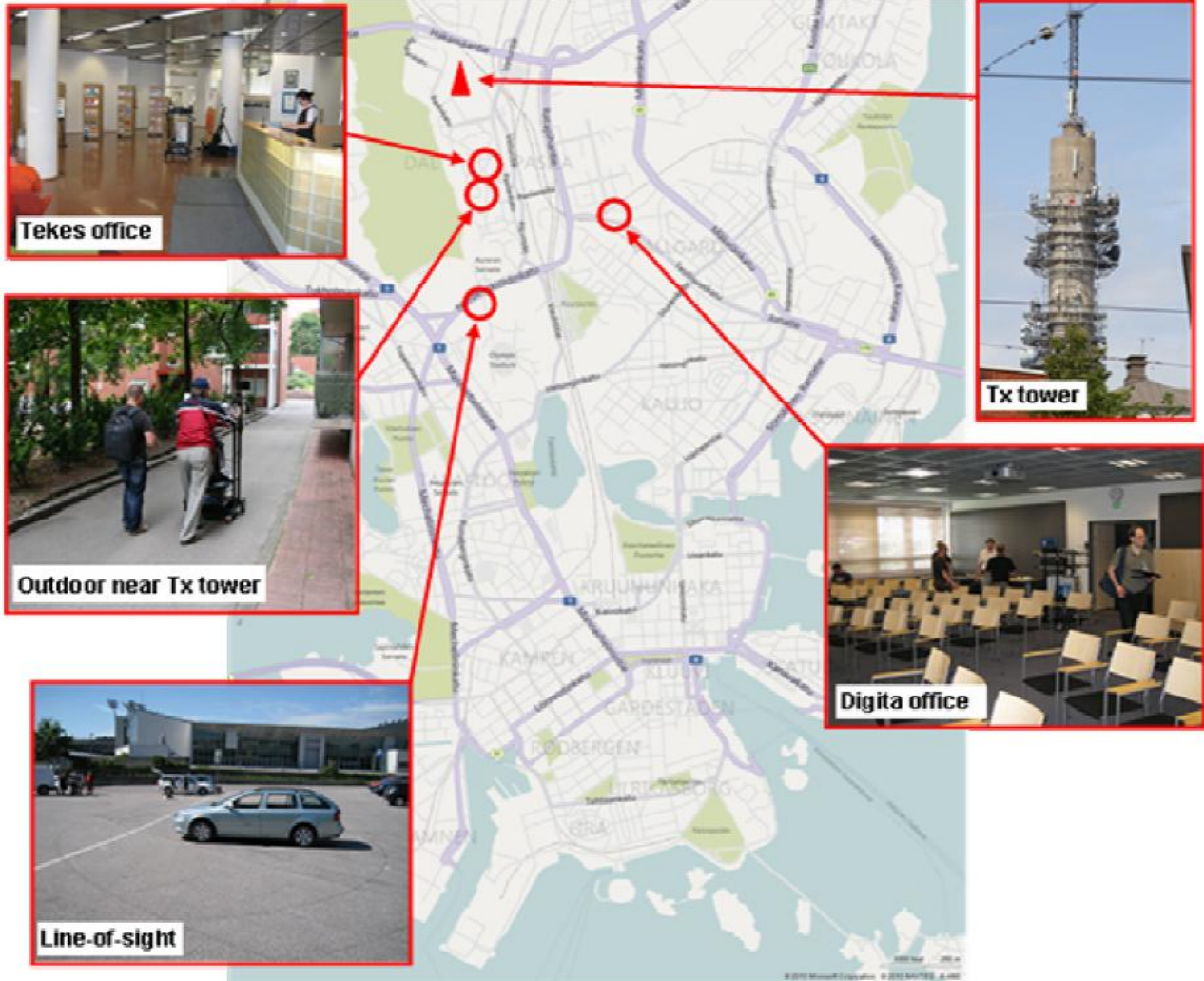


Figure 1: Locations where measurements were taken

3.2 Block Diagram Setup

The equipment for the channel sounding was contributed by several partners and the setup can be summarised in the block diagram as shown in Figure 2. The main equipment contributors are as follows:

- | | |
|------------------------------------|--------------|
| 1. Modulator | : BBC R&D |
| 2. Power Amplifier | : Digita Oy |
| 3. Transmit antennas | : Digita Oy |
| 4. Application antennas : | |
| a. Amphenol | |
| b. BBC | |
| c. Nokia | |
| d. TUAS (x2) | |
| 5. Channel Recorder (data capture) | : Elektrobit |
| 6. MIMO Receiver (channel display) | : BBC R&D |

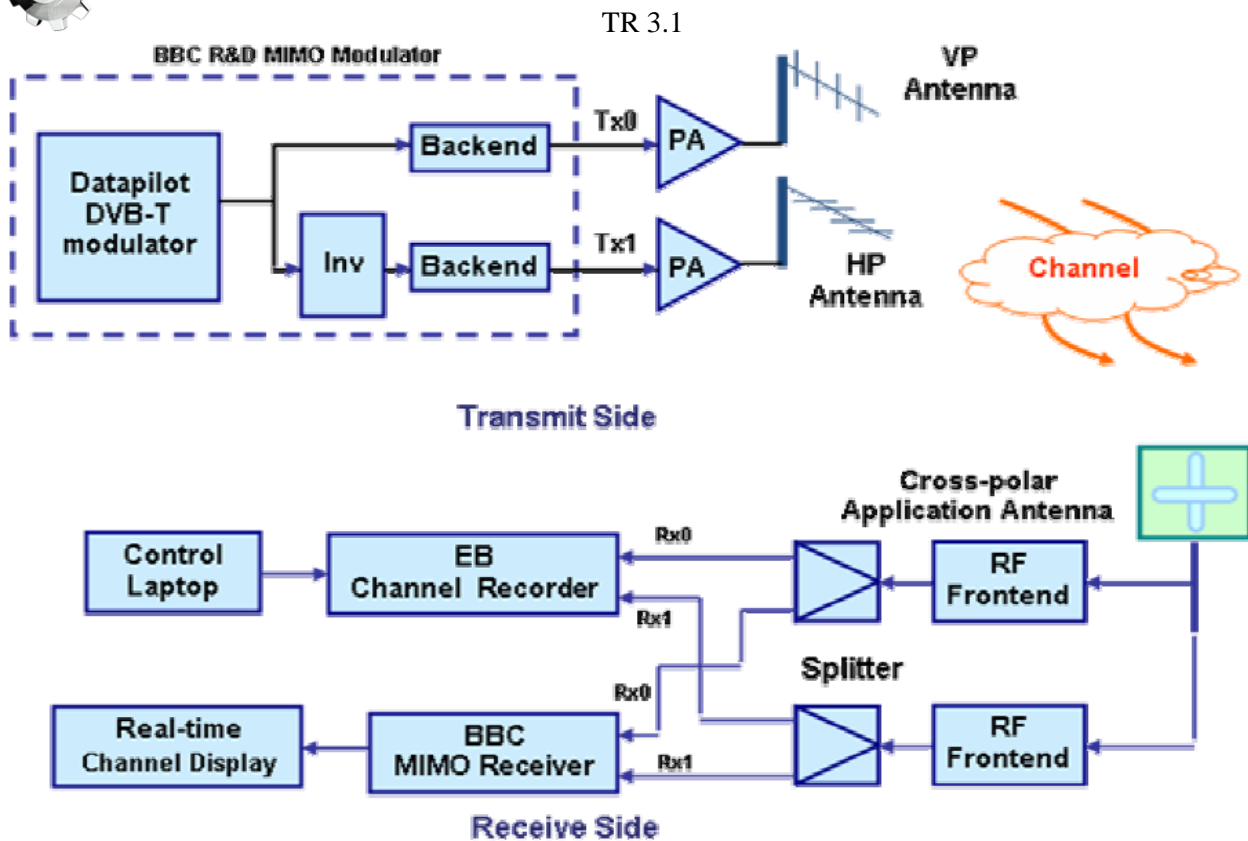


Figure 2: Block diagram of channel sounding setup

3.3 Application Antennas

Five application antennas (referred to APP1, APP2, APP3, APP4 and APP5 during the campaign) were used with Elektrobit's data capture receiver to record the channel. These antennas were provided by Amphenol, Nokia, TUAS and BBC as stated earlier.

3.4 Transmitter

The Pasila Tower was used to transmit the data pilots in both the horizontal and vertical polarized plane. It is situated at the north of the city as indicated in Figure 1. The horizontal and vertical antennas mounted on the transmitting tower are shown in Figure 3. This transmitting tower is approximately 146m above ground level with the technical equipment located at the height of 112m.

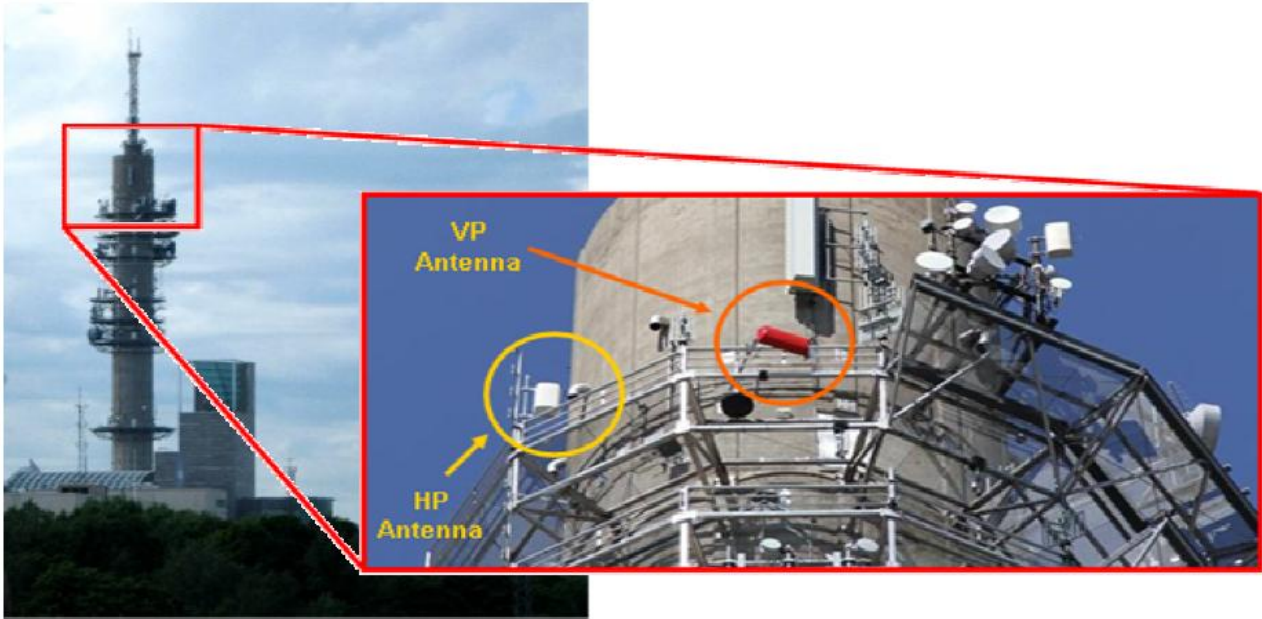


Figure 3: Transmitter tower (Pasila)

3.5 Modulator

The modulator's firmware has been programmed to output pilot data as described in the signal chapter 2. This system is basically based on DVB-T specification with the data carriers modulated in a predefined long PRBS sequence. The PRBS has a sequence length of $2^{23}-1$ with the generator polynomial $X^{23}+X^{18}+1$. The equipment setup inside the transmitting tower is shown in Figure 4. The output of the power amplifiers were checked to ensure equal power output. It was recorded during the campaign that the output power from the amplifiers are +41.6 dBm.

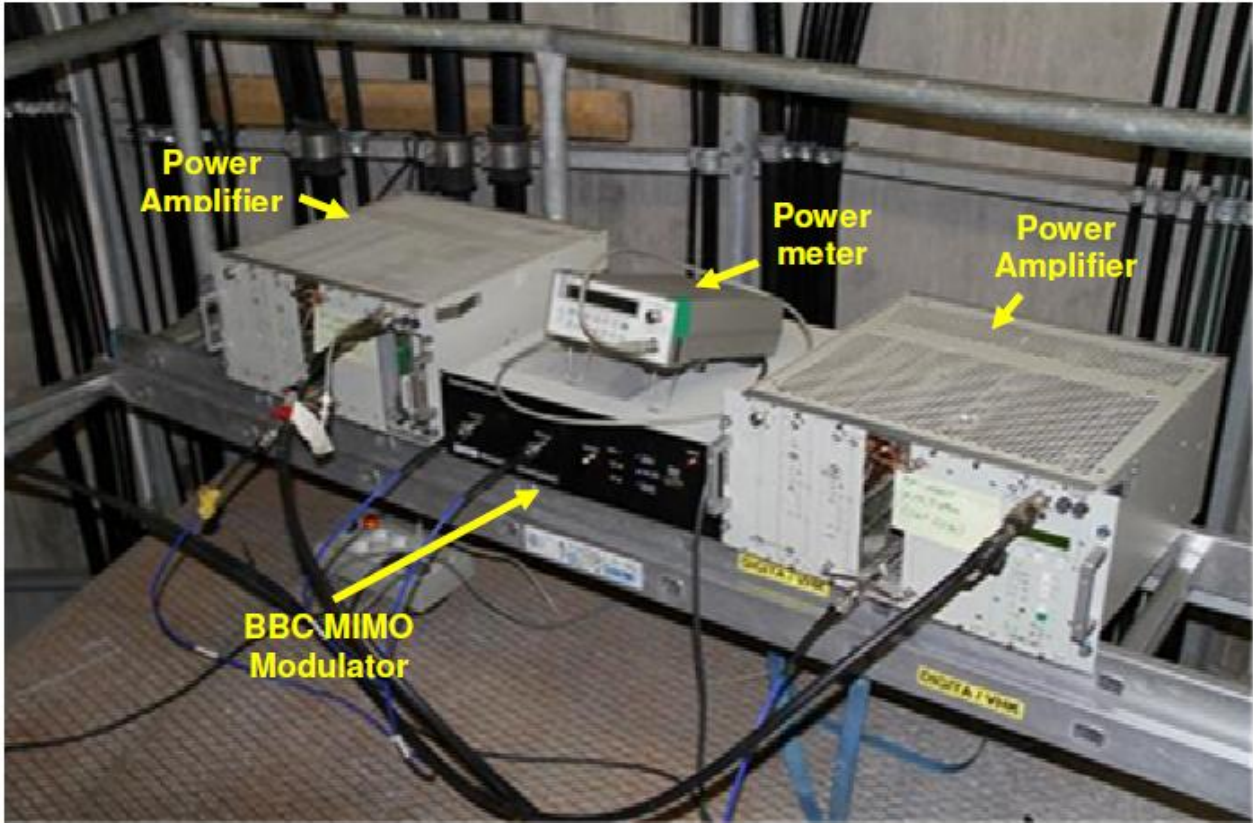


Figure 4: Modulator setup inside the transmitting tower

3.6 Coverage prediction

The individual coverage prediction for the horizontal and vertical antennas at 1.5m above ground is shown in Figure 5. The horizontal panel antenna was able to cover all the locations specified in this sounding campaign, however the vertical antenna has a much narrower beam-width and hence a panning mechanism was built into the VP antenna setup.

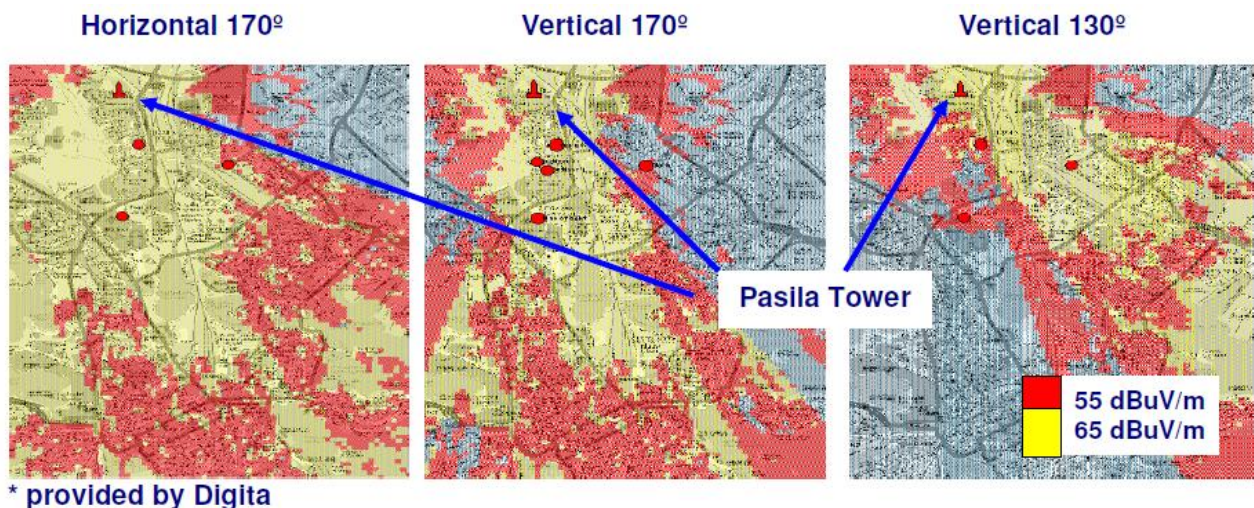


Figure 5: Coverage prediction on both the horizontal and vertical antennas

3.7 Portable Receiver (for data capture)

The portable receiving station was put together as shown in Figure 6 and it consists of the Elektrobit channel recorder (connected to the control laptop), BBC MIMO receiver with real-time channel display, cross-polar application antenna and batteries to power up all the equipment. All these were mounted on a push trolley

and the application antenna was mounted on an ‘extended-arm’ to minimize interference from the equipment. The antenna was about 1.5 meters above ground. The real-time channel display was very useful to give an instant feedback of the channel response and to ensure the integrity of the captured data.

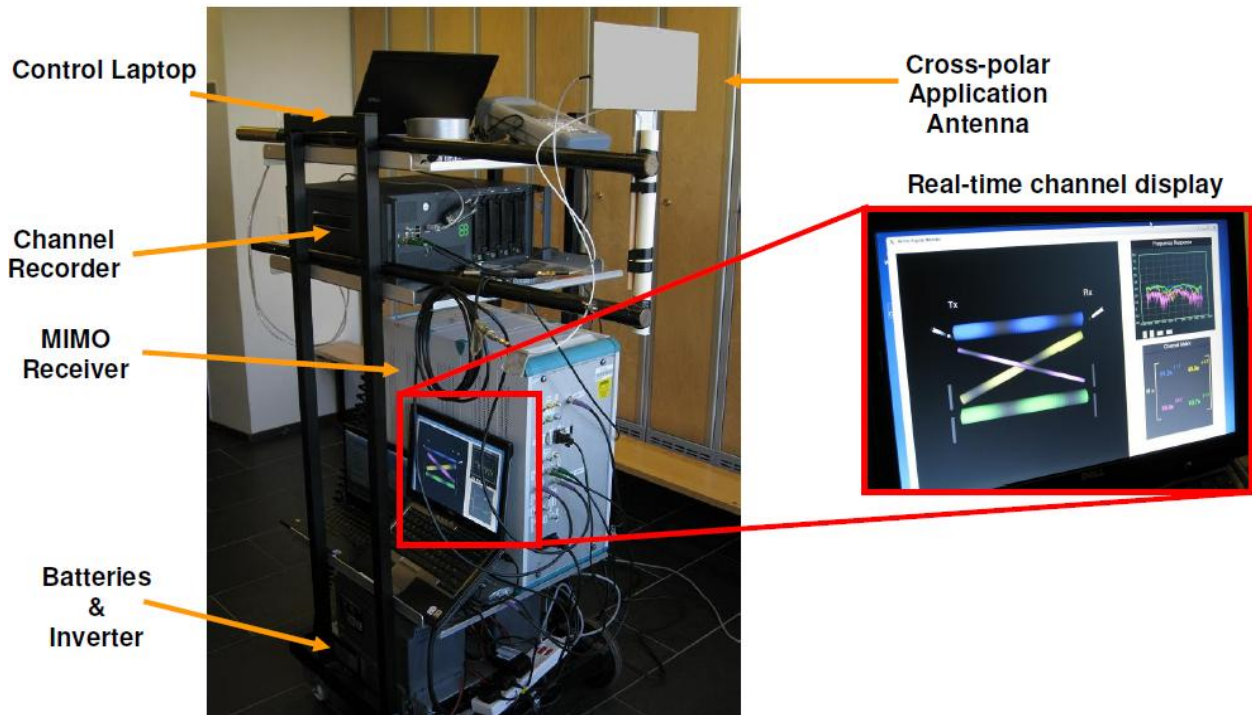


Figure 6: Portable receiving station

3.8 Campaign Schedule

The channel sounding campaign schedule is as follow:

- Day 1 (28th June 2010)
 - Sounding campaign planning
 - Equipment setup and check
 - Rebuilding of real-time receiver
 - Basic setup test inside Digita office
- Day 2 (29th June 2010)
 - Real measurement recording in Digita office
 - Measurement outside Digita office
- Day 3 (30th June 2010)
 - Calibration
 - Measurement at Olympic stadium car park
 - Indoor & outdoor measurement at the Tekes office
- Day 4 (1st July 2010)
 - Strong non-line-of-sight (NLOS) outdoor measurement near Pasila tower / Tekes office
 - Dismantling setup
- Day 5 (2nd July 2010)
 - Packing and calibration by Elektrobit

At every location, the data capture receiver will follow a specified route where it was repeated with all the five application antennas. At every location, a 6th run was done with the first application antenna mounted in order to check if there are any anomalies during the measurement runs.

3.9 Channel models

After collecting all the sounding data, the BBC R&D was heavily involved in processing the data to create the necessary channel models for DVB-NGH. Electrobit, Digita and Tampere University assisted in the initial stages of post-processing while Technische Universität Braunschweig (TU-BS) provided valuable input to the refinement and validation of the channel model. There are also other contributors from the TM-H group in the final Helsinki2 Channel Models document [2].

After analysing all the data, it was proposed that there will be two channel models; Portable Indoor (PI) and Portable Outdoor (PO), for the MIMO configuration in DVB-NGH. The full description of the channel models proposed will be presented in the next chapter.

4 DEFINED CHANNEL MODELS (DVB-NGH CHANNEL MODELS)

This chapter describes the channel models which are intended to be used in the development process of the DVB-NGH digital broadcasting standard. The models are created on the basis of the measurements presented here. The text for the terrestrial channel models is Compiled by Peter Moss (BBC). Contributions to the material are made by Mihail Petrov, Joerg Robert, Pekka Talmola, Erik Stare, Volker Pauli, Danish Nisar, Ismael Gutierrez, Alain Mourad and Peter Moss. The satellite and hybrid channel model presented here is created based on the measurements performed by CNES.

The target is to give common definitions of channel models for all who will use them in simulations and laboratory measurements. A variety of models are included to cover a wide range of reception conditions. Also included are specific channel definitions for testing receiver synchronization issues in SFN-conditions.

The terrestrial models are intended to be representative of UHF band reception (approximately 500-1000MHz). The terrestrial MIMO section of this chapter includes revisions resulting from the 2010 Helsinki channel sounding campaign.

4.1 Single-Input-Single-Output (SISO) Channel models

4.1.1 Stationary reception

Gaussian channel

In this channel model only white Gaussian noise (AWGN) is added to the signal, and there is only one time-invariant path.

Simple two path profile, 0dB echo

This profile only includes two paths. Each path, '*i*', is defined by α_i , τ_i , Δf_i which denote the amplitude, delay and frequency shift of the particular path '*i*', respectively. The profile parameters are given in [Table 1](#).

Table 1: 0 dB Echo profile

i	α_i (dB)	τ_i (μ s)	Δf_i (Hz)
1	0	0	0
2	0	0.9 Δ	1

For a system based on COFDM with a guard interval, the parameter ' Δ ' denotes the guard interval duration in μ s. For other systems, it is the stated maximum delay tolerance of the system.

4.1.2 Portable reception

MIMO-model based

For simulation of portable SISO reception, the path $h_{1,1}$ taken from the MIMO portable channel definitions shall be used.

4.1.3 Mobile Reception

Two SISO models are defined, one based on the MIMO model described below and the other based on the TU6 model

MIMO-model based

In this case mobile SISO reception is defined as the path $h_{1,1}$ taken from the MIMO mobile channel.

TU6 Model

This profile reproduces the terrestrial propagation in an urban area. It has been defined by COST 207 as a typical urban (TU6) profile and is made of 6 paths having wide dispersion in delay and relatively strong power. The profile parameters are given in Table 2.

Table 2: Typical Urban profile (TU6)

Tap number	Delay (μ s)	Power (dB)	Doppler Spectrum
1	0.0	-3	Classical
2	0.2	0	Classical
3	0.5	-2	Classical
4	1.6	-6	Classical
5	2.3	-8	Classical
6	5.0	-10	Classical

where the Classical Doppler spectrum is defined as:

$$K(f; f_D) = \frac{1}{\sqrt{1 - (f/f_D)^2}}$$

The Doppler width parameter should be assigned values corresponding to 60km/h and 350km/h at 600MHz; i.e. **33.3Hz** and **194.8Hz**.

Mobile TU6-based SFN

This profile reproduces the terrestrial propagation in an urban area in a Single Frequency Network (SFN). Each transmitter in the SFN is modelled as one independent TU6 profile and the total Mobile SFN channel is therefore the sum of all individual and independent TU6 channel models, each having a unique level and delay. A frequency shift shall also be introduced in each test path as detailed below.

One particular TU6 profile, i.e. the received paths originating from one particular transmitter, is denoted $\alpha_i \text{TU6}(\tau_i)$, where α_i and τ_i are the amplification and delay constants to be applied to all individual paths of that particular TU6 profile. In the special case with only one transmitter the values of α_i and τ_i are set to unity and zero respectively.

The general mobile SFN channel profile, SFN-TU6, with N transmitters can be described in the following way:

$$\text{SFN-TU6} = \sum_{i=1}^N \alpha_i \text{TU6}(\tau_i)$$

In a real SFN almost any values of α_i and τ_i may appear, τ_i values however being limited by the size of the SFN. Also the value of N may vary a lot depending on SFN, although the actual number of transmitters to be considered in the channel profile modelling may depend on the particular network design and receiver performance.

Important special cases of this general model are the cases with two or three transmitters, i.e. the cases N=2 and N=3 with wide variations of α_i and τ_i values. In case of “classical OFDM” the parameter Δ denotes the guard interval length; in a non-OFDM system it would correspond to the specified maximum delay tolerance of the system.

Two transmitter test profile (N=2)

$$\tau_1 = 0 \mu\text{s}, \tau_2 = \{0.05\Delta, 0.9\Delta\} \Delta f_1 = 0 \Delta f_2 = +2\text{Hz}$$

$$\alpha_1 = 0 \text{ dB}, \alpha_2 = \{0, -3, -6, -9\} \text{ dB} \quad (\text{“post echo” case})$$

$$\alpha_2 = 0 \text{ dB}, \alpha_1 = \{0, -3, -6, -9\} \text{ dB} \quad (\text{“pre echo” case})$$

Three transmitter test profile (N=3)

$$\Delta f_1 = 0 \Delta f_2 = +2\text{Hz} \Delta f_3 = -2\text{Hz}$$

1st TU6 (“Pre echo”)

$$\alpha_1 = \{0, -3, -6, -9\} \text{ dB}$$

$$\tau_1 = -0.45\Delta$$

2nd TU6 (“Main signal”)

$$\alpha_2 = 0 \text{ dB}$$

$$\tau_2 = 0 \mu\text{s}$$

3rd TU6 (“Post echo”)

$$\tau_3 = 0.45\Delta$$

$$\alpha_3 = \{0, -3, -6, -9\} \text{ dB}$$

Note: α_1 and α_3 values to be varied independently.

4.2 Multiple-Input-Multiple-Output (MIMO) Channel models

4.2.1 General approach

The aim is to provide a time-domain model of paths shown as $h_{11}, h_{12}, h_{21}, h_{22}$ in the figure below, where Tx1 and Tx2 represent a cross-polar pair of antennas at a terrestrial transmitter site and Rx1 and Rx2 the two elements of a MIMO receive antenna whether fixed or mobile.

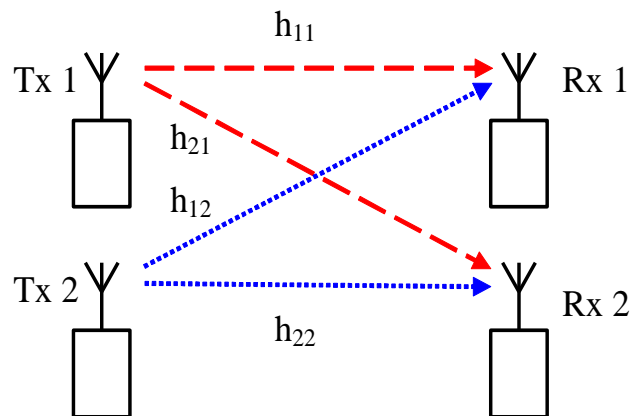


Figure 7: 2-by-2 MIMO system

The two proposed models, outdoor portable and indoor portable, will now be described.

4.2.2 Outdoor portable model

An 8-tap model of the propagation paths is proposed. The delays and relative power gains of the direct paths h_{11}, h_{22} are tabulated below in Table 1. Taken together with the cross-polar terms h_{12}, h_{21} the sum of the tap powers is unity (0dB).

Table 3: Power delay profile of the 8-tap outdoor model.

Tap number, p	Excess delay, τ_p (μs)	Co-polar power gain $\sigma_{11}(\tau_p)^2 = \sigma_{22}(\tau_p)^2$ (dB)
1	0	-4.0
2	0.1094	-7.5
3	0.2188	-9.5
4	0.6094	-11
5	1.109	-15
6	2.109	-26
7	4.109	-30
8	8.109	-30

When used in a discrete baseband model, the excess delays will be rounded to integer sample periods. For instance, in the case of an 8 MHz bandwidth the sample period T is 7/64 us and the resulting discrete excess delays are 0, 1, 2, 6, 10, 19, 38, and 74 samples.

The cross-polar discrimination (XPD) is defined as the ratio of the co-polarized average received power to the cross-polarized average received power. XPD quantifies the separation between the two cross-polarized channels. The larger the XPD, the less energy is coupled between the cross-polarized channels.

The XPD for outdoor and indoor reception takes the following values:

Table 4: Cross-polar discrimination for outdoor reception.

Environment	XPD (linear scale)	XPD (log scale)
Outdoor	4	6 dB

The reciprocal XPD factor w^2 for tap p is defined as $w^2 = \sigma_{12}^2(\tau_p) / \sigma_{11}^2(\tau_p) = \sigma_{21}^2(\tau_p) / \sigma_{22}^2(\tau_p)$.

The time-variant channel model for the link between TX antenna n and RX antenna m can be written as:

$$h_{mn}(t, \tau) = \sum_{p=1}^{N_p} g_{mn}(t, \tau_p) \delta(\tau - \tau_p) \quad (2)$$

Where t is time index, τ the delay index, N_p ($= 8$) the number of paths, τ_p the p -th excess delay ($\tau_1 = 0$), and $g_{mn}(\tau_p, t)$ the p -th time-variant complex-valued gain.

A 2x2 time-variant matrix \mathbf{H} is then defined as:

$$\mathbf{H}(t, \tau) = \begin{bmatrix} h_{11}(t, \tau) & h_{12}(t, \tau) \\ h_{21}(t, \tau) & h_{22}(t, \tau) \end{bmatrix} \quad (3)$$

Outdoor portable parameters

In the outdoor portable environment, the XPD is 4, as tabulated in Table 4.

For the **first tap** τ_1 , the complex-valued gain is purely LOS:

$$g_{mn}(t, \tau_1) = [\sigma_{mn}(\tau_1) \exp(j\theta_{mn})] \dots (m = n) \quad (4A)$$

$$g_{12}(t, \tau_1) = [\sigma_{12}(\tau_1) \exp(j(\theta_{12} + 4\pi t))] \quad (4B)$$

$$g_{21}(t, \tau_1) = [\sigma_{21}(\tau_1) \exp(j(\theta_{21} - 4\pi t))] \quad (4C)$$

- The overall K-factor of the outdoor model (K_0) is 1.0
- θ_{mn} are the initial phases of the LOS component. They are real-valued i.i.d. random variables uniformly distributed in the interval $[0, 2\pi)$. The LOS components of the direct terms ($n=m$) have no Doppler shift, whereas for cross-terms a shift of $\pm 2\text{Hz}$ is specified.
- $w^2 = 0.25$

For the **remaining taps** ($p = 2 \dots 8$), only NLOS component is assumed, as expressed below:

$$g_{mn}(t, \tau_p) = \varphi_{pmn}(t) \quad (5)$$

- $w^2 = 0.25$
- $\varphi_{pmn}(t)$ are the time-variant random components of the tap, which model the Doppler spread. They are complex-valued zero-mean Gaussian processes having a combination of a Jakes spectrum and a fixed frequency offset and exhibiting intra-tap correlation. The vector $\varphi_p(t) = [\varphi_{p11}(t) \ \varphi_{p12}(t) \ \varphi_{p21}(t) \ \varphi_{p22}(t)]^T$ is specified to have the following covariance matrix at the p^{th} tap:

$$\mathbf{R}_p = \sigma_{11}^2(\tau_p) \begin{pmatrix} 1.00 & 0.06 & 0.06 & 0.05 \\ 0.06 & 0.25 & 0.03 & 0.05 \\ 0.06 & 0.03 & 0.25 & 0.06 \\ 0.05 & 0.05 & 0.06 & 1.00 \end{pmatrix} \quad (6)$$

The Cholesky decomposition can be used to provide a transition matrix to pre-multiply a 4-element i.i.d. vector at each tap to create the above autocorrelation properties. A suitable matrix is

$$\mathbf{V} = \begin{pmatrix} 1.00 & 0 & 0 & 0 \\ 0.06 & 0.4964 & 0 & 0 \\ 0.06 & 0.0532 & 0.4935 & 0 \\ 0.05 & 0.0947 & 0.1053 & 0.9887 \end{pmatrix} \quad (7)$$

N.B. Using the matrix \mathbf{V} does not remove the need for the term $\sigma_{11}^2(\tau_p)$

The Jakes spectrum $S(f, f_d)$ is characterized by the following equation:

$$S(f, f_d) = \frac{1}{\pi f_d \sqrt{1 - \left(\frac{f}{f_d}\right)^2}} \quad \forall f \in]-f_d, f_d[; = 0 \quad \text{elsewhere} \quad (8)$$

Where f_d is the maximum Doppler frequency, which is chosen to be proportional to an assumed vehicle speed v . In (8), f_d is strictly greater than 0.

The typical receiver velocities we consider for outdoor portable reception are **0km/h** and **3 km/h**. At a carrier frequency of 600 MHz the resulting Doppler frequency f_d is **1.67 Hz**.

The spectrum of the p^{th} tap is shown in the table below:

Table 3: Tap spectral characteristics of the 8-tap outdoor model.

Tap number, p	
1	LOS only, no additional Doppler shift
2	$S\left(f - \frac{3f_d}{4}, \frac{f_d}{4}\right)$
3	$S\left(f - \frac{3f_d}{4}, \frac{f_d}{4}\right)$
4	$S\left(f + \frac{3f_d}{4}, \frac{f_d}{4}\right)$
5	$S\left(f + \frac{3f_d}{4}, \frac{f_d}{4}\right)$
6	$S\left(f + \frac{3f_d}{4}, \frac{f_d}{4}\right)$
7	$S\left(f + \frac{3f_d}{4}, \frac{f_d}{4}\right)$
8	$S\left(f + \frac{3f_d}{4}, \frac{f_d}{4}\right)$

4.2.3 Indoor portable model

An 8-tap model of the propagation paths is again proposed. The delays and relative power gains of direct paths h_{11}, h_{22} are tabulated below in Table 4. Taken together with the cross-polar terms h_{12}, h_{21} the sum of the powers is unity (0dB).

Table 4: Power delay profile of the 8-tap indoor model.

Tap number, p	Excess delay, τ_p (μ s)	Co-polar power gain $\sigma_{11}^2 = \sigma_{22}^2$ (dB)
1	0	-6.0
2	0.1094	-8.0
3	0.2188	-10
4	0.6094	-11
5	1.109	-16
6	2.109	-20
7	4.109	-20
8	8.109	-26

The XPD for outdoor and indoor reception takes the following values:

Table 5: Cross-polar discrimination for outdoor reception.

Environment	XPD (linear scale)	XPD (log scale)
Indoor	1.78	2.5 dB

Indoor portable parameters

For the **first tap** τ_1 , the complex-valued gain is split into two components, LOS and NLOS. This writes as:

$$g_{mn}(t, \tau_1) = \left[\underbrace{\sigma_{mn}(\tau_1) \sqrt{\frac{K}{1+K}} \exp(j\theta_{mn})}_{LOS} + \underbrace{\sqrt{\frac{1}{1+K}} \varphi_{1mn}(t)}_{NLOS} \right] \dots (m = n) \quad (4A)$$

$$g_{12}(t, \tau_1) = \left[\underbrace{\sigma_{12}(\tau_1) \sqrt{\frac{K}{1+K}} \exp(j\theta_{12}) \exp(j4\pi t)}_{LOS} + \underbrace{\sqrt{\frac{1}{1+K}} \varphi_{112}(t)}_{NLOS} \right] \quad (4B)$$

$$g_{21}(t, \tau_1) = \left[\underbrace{\sigma_{21}(\tau_1) \sqrt{\frac{K}{1+K}} \exp(j\theta_{21}) \exp(-j4\pi t)}_{LOS} + \underbrace{\sqrt{\frac{1}{1+K}} \varphi_{121}(t)}_{NLOS} \right] \quad (4C)$$

- The overall K-factor of the indoor model (K_0) is approximately 0.2
- K, the Ricean-K factor for the first tap is 1
- $w^2 = 0.56$
- Note that $\varphi_{pmm}(t)$ exists in the indoor model for $p=1$ as well as $p=2-8$.

The indoor covariance matrices (for taps 2-8 and the NLOS part of tap 1) are defined as

$$\mathbf{R}_p = \sigma_{11}^2(\tau_p) \begin{pmatrix} 1.00 & 0.15 & 0.10 & 0.15 \\ 0.15 & 0.56 & 0.06 & 0.04 \\ 0.10 & 0.06 & 0.56 & 0.15 \\ 0.15 & 0.04 & 0.15 & 1.00 \end{pmatrix} \quad (9)$$

A suitable transition matrix for the indoor case is

$$\mathbf{V} = \begin{pmatrix} 1.00 & 0 & 0 & 0 \\ 0.15 & 0.7331 & 0 & 0 \\ 0.10 & 0.0614 & 0.7391 & 0 \\ 0.15 & 0.0239 & 0.1807 & 0.9717 \end{pmatrix} \quad (10)$$

The typical receiver velocities we consider for indoor portable reception are **0km/h** and **3 km/h**. At a carrier frequency of 600 MHz the resulting Doppler frequency f_d is **1.67 Hz**.

The spectrum of the p^{th} tap is shown in the table below:

Table 6: Tap spectral characteristics of the 8-tap indoor model.

Tap number, p	
1 (NLOS component)	$S(f, f_d)$
2	$S\left(f - \frac{3f_d}{4}, \frac{f_d}{4}\right)$
3	$S\left(f - \frac{3f_d}{4}, \frac{f_d}{4}\right)$
4	$S\left(f + \frac{3f_d}{4}, \frac{f_d}{4}\right)$
5	$S\left(f + \frac{3f_d}{4}, \frac{f_d}{4}\right)$
6	$S\left(f + \frac{3f_d}{4}, \frac{f_d}{4}\right)$
7	$S\left(f + \frac{3f_d}{4}, \frac{f_d}{4}\right)$
8	$S\left(f + \frac{3f_d}{4}, \frac{f_d}{4}\right)$

4.2.4 Additional antenna rotation and asymmetry terms

The following applies to both outdoor and indoor models.

In deriving the antenna-specific data from which the model parameters were derived, the raw data was rotated by up to $\pm 40^\circ$ to find the angle which maximised the cross-polar discrimination. This was to correct for both physical mounting differences and antenna axis differences with respect to the casing. It also ensured averaging across antennas retained legitimacy in terms of cross-polar discrimination.

However in practice this ‘ideal’ alignment may not be representative and so a further rotation matrix \mathbf{W} , with angle Ω chosen from the set $\{-45^\circ, 0^\circ, +45^\circ\}$ is recommended with the angle fixed for a particular simulation run.

In addition, an asymmetry matrix $\mathbf{\Gamma}$ is included to model observed H/V asymmetries which persist over many contiguous channel realisations (typically over 10m). $\mathbf{\Gamma}$ should also be taken as fixed for a particular simulation run. It takes values from the set

$$\left\{ \begin{bmatrix} 1.1074 & 0 \\ 0 & 0.8796 \end{bmatrix}, \begin{bmatrix} 1 & 0 \\ 0 & 1 \end{bmatrix}, \begin{bmatrix} 0.8796 & 0 \\ 0 & 1.1074 \end{bmatrix} \right\}.$$

The resulting channel matrix $\mathbf{H}_c(t, \tau)$ is hence derived from $\mathbf{H}(t, \tau)$ as follows:

$$\mathbf{H}_c(t, \tau) = \mathbf{W}\mathbf{H}(t, \tau)\mathbf{\Gamma} = \begin{bmatrix} \cos \Omega & -\sin \Omega \\ \sin \Omega & \cos \Omega \end{bmatrix} \begin{bmatrix} h_{11}(t, \tau) & h_{12}(t, \tau) \\ h_{21}(t, \tau) & h_{22}(t, \tau) \end{bmatrix} \begin{bmatrix} \Gamma_{11} & 0 \\ 0 & \Gamma_{22} \end{bmatrix} \quad (11)$$

4.2.5 Simulation practicalities

Updating LOS phases, \mathbf{W} and $\mathbf{\Gamma}$

The LOS phases θ_{mn} and parameters \mathbf{W} and $\mathbf{\Gamma}$ are both intended to be fixed for periods of five seconds before re-initialisation. This can be relaxed if the time-interleaving length of the system is considerably shorter than this such that no material change in the results would be expected. Indeed, re-initialising per TI frame is acceptable if it is clear this is equivalent to the longer runs. Sudden changes of parameters during OFDM blocks should be avoided however.

Furthermore, regarding matrix \mathbf{W} , if it is clear that the angles $+45^\circ$ and -45° give the same result in a particular scheme, the requirement to do both can be dropped.

4.2.6 Generating fixed channel realizations (0Hz Doppler snapshots)

If we simulate a time-invariant channel, i.e. $f_d = 0$, the Doppler shift for the LOS components and the Doppler spreads for the NLOS components are not modelled. Instead, it suffices to generate a number of independent realizations.

For each LOS component we generate four real-valued i.i.d. phases θ_{mn} with uniform distribution. For the NLOS components we need to generate four complex-valued variables φ_{pmm} with the prescribed intra-tap correlation properties.

4.2.7 Mobile vehicular outdoor model

For the mobile case, we use the outdoor model and consider two receiver velocities: **60 km/h** and **350 km/h**. At a carrier frequency of 600 MHz the resulting Doppler frequencies f_d are **33.3 Hz** and **194.8 Hz** respectively.

4.2.8 4 x 2 model (& 2-tower SFN)

A pair of uncorrelated 2 x 2 models should be invoked, one of which has a time offset taken from $\{0.05\Delta, 0.9\Delta\}$

where Δ denotes the guard interval length for an OFDM system. In a non-OFDM system it would correspond to the specified maximum delay tolerance of the system.

The time-shifted element should additionally have a fixed frequency offset of +1.0Hz.

A second parameter is the power ratio between the signals received from the two towers, which models the power imbalance. Suggested values are {0, -3, -6, -9} dB.

4.3 Satellite and hybrid channel models

Within ENGINES and DVB-NGH working group, various models are available for S-band propagation channels including a satellite segment:

- hybrid propagation channel software (mainly empirical for both the satellite and the terrestrial segments)
- SISO and MIMO physical model for tree shadowed environment (including nomadic effects)
- SISO and MIMO empirical model for various environments.

A detailed description and a critical analysis of these models (and their associated softwares) are presented in this section. Such generative model are quite different from typical terrestrial reference propagation models: the Land Mobile Satellite (LMS) propagation channel at S-band is generally assumed to be locally Ricean with Rice parameters varying quite rapidly (typically every meter) along a travelled path. Indeed, the LMS propagation channel is made of interactions with very few obstacles shadowing the Rx-Tx link which explains this quite fast fluctuation that must be considered when assessing air interface performances. The models described in this section all include such time/space variations of Rice parameters. Nevertheless they could also be used to infer simpler reference Rice models suitable only for small scale analyses over the LMS propagation channel. Such a complexity reduction is not addressed in this document.

4.3.1 Hybrid channel software

4.3.1.1 SISO hybrid propagation channel

This software relies mainly on hybrid measurements carried out by CNES in 2008 in the vicinity of a small-sized French city, Auch (about 22000 inhabitants), at S-band. Details concerning the Single Frequency Network (SFN) terrestrial segment and the Land Mobile Satellite (LMS) segment soundings are given respectively in [3] and [4]. Main features of these hybrid measurements are given on Table 5.

Measurement characteristics		Terrestrial segment	“Satellite” segment
Tx characteristics	Number of Tx	2 (spaced out by about 1 km: “Workshop” and “Train station”)	2 * (collocated on board an helicopter)
	Link frequency	2177.5 MHz	2172.5 MHz
	Height above ground level	≈ 15 m (≈ macrocell configuration)	≈ 2600 m
	Elevation angle to Rx		35°
	Azimuth angle to Rx		40°
	RF power	≈ 20 W	≈ 20 W
	Antenna gain	17 dBi (4 antennas per site)	≈ 0 dBi (for elevation = 35°)
	Antenna polarization	Vertical	RHCP & LHCP
Rx characteristics	Number of Rx antennas	2 dipoles * (spaced out by about 11.5 cm)	
	Antenna gain	2 dBi	0 dBi
	Antenna polarization	Vertical	
	Sounding method	Wideband (complex CIR)	Narrowband (Rx power)
	Measurement bandwidth	5 MHz	100 kHz
	Sampling distance ($\lambda \approx 13.8$ cm)	15.6 cm	3.5 cm
Environments (all suburban)	work (industrial)⇒ home (house) (Tv1a<)	Total distance ≈ 15.8 km	
	home (house)⇒ work (office) (Tv1b)		
	home (block of flats)⇒ work (industrial) (Tv1d<)		
	work (office)⇒ home (block of flats) (Tv1c)		

* Note: Only SISO results are used in the hybrid software

Table 5: Auch 2008 hybrid measurements main characteristics

Specific post processing was applied to measured datasets:

- Data calibration: Line Of Sight level correction for “satellite” link data, bias and offset removal for terrestrial links data
- Assessment of software input parameters:
 - Satellite link: Ricean small-scale fitting providing both the direct path amplitude $a(t)$ and the multipath amplitude $\sigma(t)$ of the propagation channel as a function of time/travelled distance (2 input parameters).
 - Terrestrial links: Assessment of the multi-taps instantaneous channel impulse response (maximum number of taps = 6 per terrestrial link). In the software, it was assumed that all terrestrial taps are Rayleigh distributed, so only the taps instantaneous multipath powers

$\{\sigma_k(t)\}_{1 \leq k \leq 6}$ and the taps delays $\{\tau_k(t)\}_{1 \leq k \leq 6}$ had to be inferred (12 input parameters for each link).

- Verification of the consistency between inferred input parameters and original datasets for terrestrial links (in particular, Delay spread, coherence bandwidth, multi-taps total power).
- Removal of periods where saturation effects happen (typically when the Rx set-up is close to a terrestrial Tx, the satellite measurement channel is generally saturated).

In the hybrid software, link budget characteristics and network temporal synchronisation are also taken into account additionally to time varying propagation channel effects. It required as input parameters:

- Satellite link: the satellite EIRP ($eirp_{Sat}$), the free space loss between the satellite, the ground terminal (fsl_{Sat}) and the receive antenna gain (g_{Sat}) and the synchronisation offset ($\tau_{0,Sat}$).
- Terrestrial links: the Tx EIRP ($eirp_{Ter}$), the receive antenna gain (g_{Ter}) and the synchronisation offset ($\tau_{0,Ter}$). Parameters can be different between the two terrestrial Tx.

Finally, starting from normalised Rayleigh distributed time series synthesised using the Zheng-Xiao model (Classical Doppler spectrum) [5], $x_{ZX}(t)$ for the satellite link or $\{x_{ZX,k}(t)\}_{1 \leq k \leq 6}$ for terrestrial links (uncorrelated processes), the hybrid software outputs for both types of links are (α = tap complex envelope, τ = tap delay):

Satellite propagation channel	Terrestrial propagation channel
$\begin{cases} \alpha_{Sat}(t) = K_0 \times (a(t) \times \exp(j2\pi f_d t + \phi_{d,0}) + \sigma(t) \times x_{ZX}(t)) \\ \tau_{Sat}(t) = \tau_{0,Sat} \end{cases}$	$\begin{cases} \alpha_{Ter,k}(t) = K_0 \times \sigma_k(t) \times x_{ZX,k}(t) \\ \tau_{Ter,k}(t) = \tau_k(t) + \tau_{0,Ter} \end{cases}, 1 \leq k \leq 6$
where $K_0 = eirp_{Sat} \times fsl_{Sat} \times g_{Sat}$ f_d and $\phi_{d,0}$ resp. the direct path Doppler shift and the direct path initial Doppler phase	where $K_0 = eirp_{Ter} \times g_{Ter}$

Concerning the Rx mobile speed $v_m(t)$ used for propagation channel emulation, three options are available for software users:

- User-defined Fixed speed
- User-defined time-varying speed
- Measured time-varying speed.

For the last option, the speed is directly inferred from CNES measurements and nothing else has to be indicated by the software user.

Actually, the output tap delays for terrestrial links are not strictly measured delays with an additional offset: depending on the selected Rx speed option, different interpolations are applied to measured delays to get the corresponding output delays. Such interpolations are also applied in the same way to other measured parameters ($a(t)$, $\sigma(t)$, $\{\sigma_k(t)\}_{1 \leq k \leq 6}$) so that the final series sampling time is fully user-defined.

This global description of the SISO hybrid channel software is summarized on Figure 8.

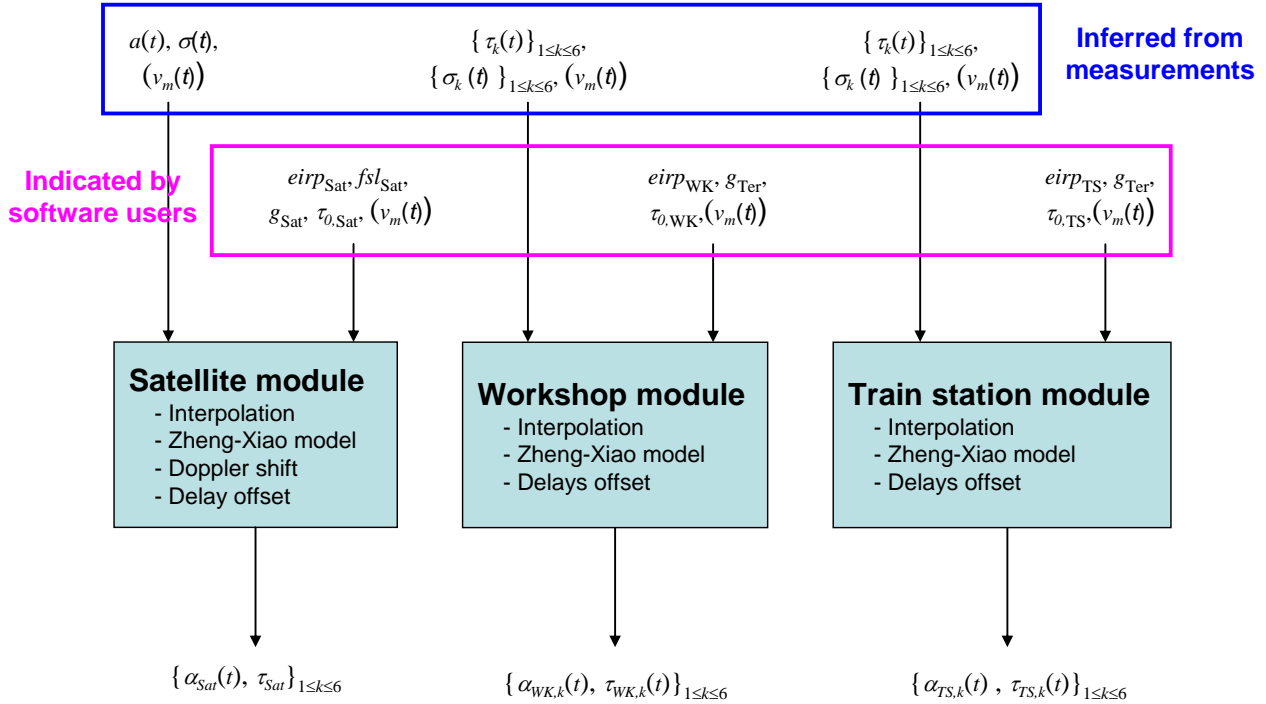


Figure 8: Hybrid propagation channel software description

An example of software outputs for the 4 environments is provided on Figure 9. It corresponds to a typical vehicular link budget with a basic synchronisation strategy:

- Satellite EIRP: 68 dBW
- Satellite free space losses: 190.6 dB
- Rx antenna gain: 4 dBi for the satellite link, -1 dBi for terrestrial links
- Satellite elevation: 35° (used to compute the synchronisation offsets $\tau_{0,Ter}$ and $\tau_{0,Sat}$ since the satellite is also assumed to be the feeder of terrestrial transmitters in this example)
- Terrestrial Tx EIRP: 25.1 dBW
- Rx speed: measured speed.

It is suggested to consider this example as a reference case for air interface simulations (which correspond to a worst case in terms of delay spread due to the synchronisation strategy).

On Figure 9, software outputs have been post-processed in such a way that the instantaneous average power (equal to the sum of the 6 taps power) can be plotted for each terrestrial link.

Warning:

The satellite channel must not be used alone for Tv1b, Tv1d & Tv1c. Indeed, when the receive set-up was close to a terrestrial transmitter, some saturation effects could happen on the satellite channel. Consequently, the corresponding periods have been removed from measurements of the satellite channel.

An example of wideband output is shown on Figure 10. It corresponds to the instantaneous power delay profile got by post-processing an instantaneous complex CIR generated by the hybrid software.

Model implementation:

The hybrid propagation channel software is implemented as a Dynamic Link Library (DLL) in particular to be compatible of various software languages. Moreover, the software generates propagation channel sample after sample meaning that it can be run continuously and does not induce any writing (and then reading in simulator) of output files. Consequently, it can be included as a module within global air interface simulators.

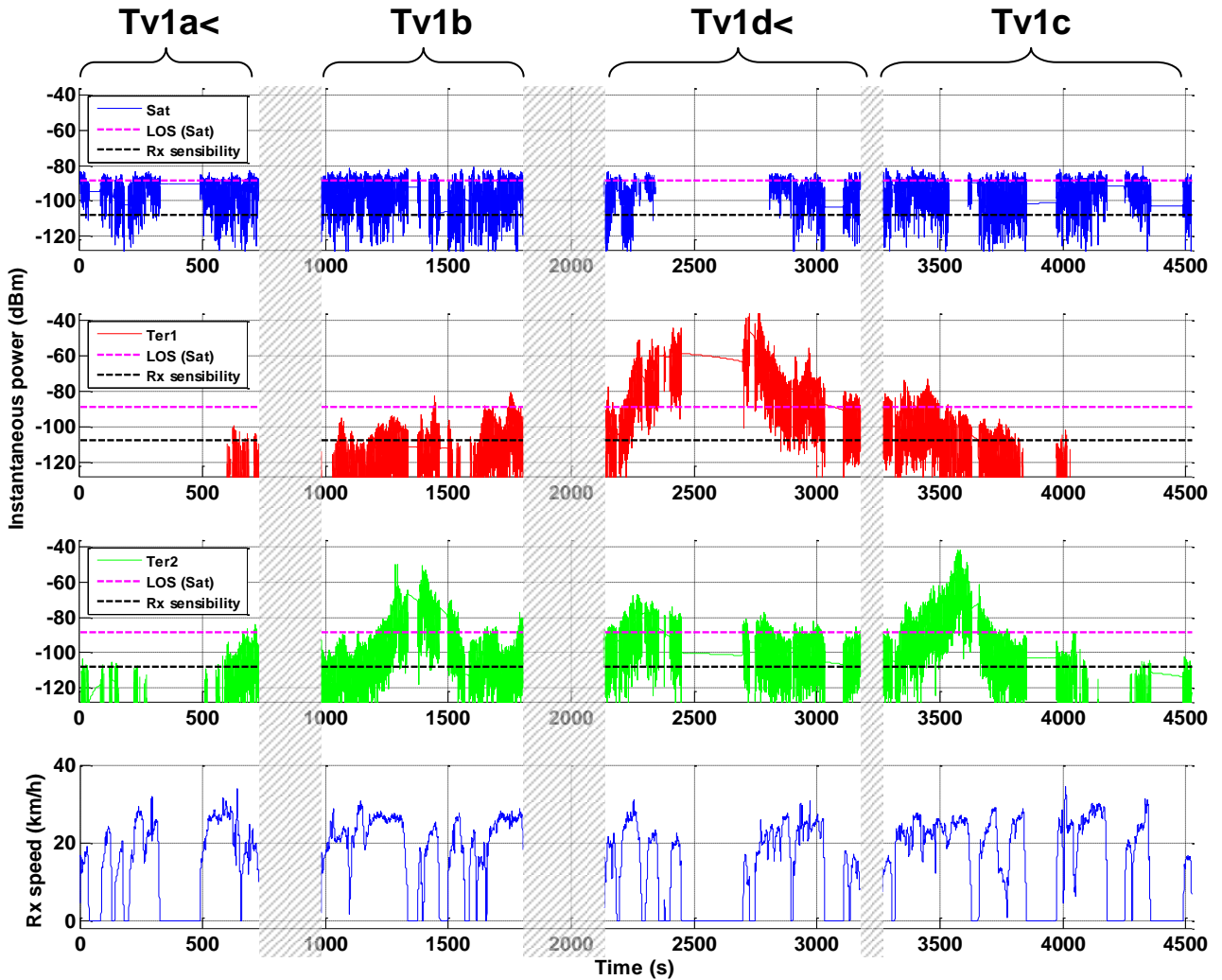


Figure 9: Example of hybrid propagation channel output (post-processed for terrestrial links)
 Rx sensibility = -107.7 dBm (vehicular)

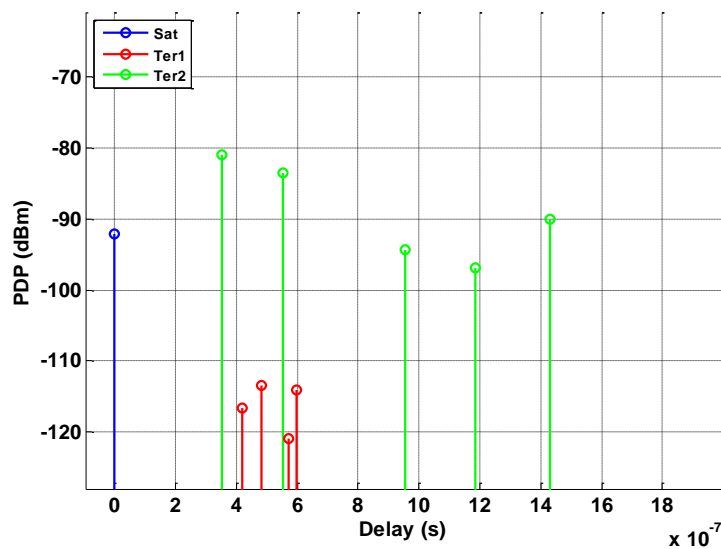


Figure 10: Example of instantaneous wideband output (complex CIR post-processed into PDP)

4.3.1.2 MIMO extension

The SISO hybrid channel has been extended using basic assumptions into a MIMO model to address the following MIMO case (MIMO channel matrix inspired from the one proposed by P.Moss (BBC)):

$$\begin{bmatrix} r_1 \\ r_2 \\ r_s \end{bmatrix} = \begin{bmatrix} M_{11} & M_{12} & \beta S_{33} \\ M_{21} & M_{22} & \beta S_{33} \\ \alpha M_{11} & \alpha M_{22} & S_{33} \end{bmatrix} \begin{bmatrix} T_1 \\ T_2 \\ T_s \end{bmatrix}$$

where

T_1, T_2 and r_1, r_2 are respectively the terrestrial transmit/receive channel terms (H and V polarisation)

T_s and r_s are respectively the satellite transmit/receive channel terms (circular polarisation)

M is the terrestrial MIMO channel submatrix (6-tap)

S_{33} is the single-tap time varying satellite channel

α is a fixed Terrestrial-Satellite antenna factor and β is a fixed Satellite-Terrestrial antenna factor.

It corresponds to the case where each terrestrial site transmits dual linearly polarized signals received by dedicated antennas at receive side and where a third antenna dedicated to the satellite is also available.

In the hybrid software, two terrestrial transmitters are included.

The underlying assumption of such a MIMO extension are the following:

- the local average powers received from a terrestrial transmitter over the two co-polar channels are equal
- the difference between the local average powers received from a terrestrial transmitter over a co-polar and a cross-polar channel are equal to the antennas cross polar discriminations XPD_{HV} and XPD_{VH}
- it is possible to fully characterize the correlation between the 4 terrestrial small scale fading processes using a single correlation matrix C_s .

With these basic assumptions, the principle to synthesise correlated MIMO channels for terrestrial links is shown on Figure 11. This method must be applied to each terrestrial tap. The $\sigma(t)$ process corresponds to the multipath amplitude of the tap generated by the hybrid software from initial data. xpd_{HV} and xpd_{VH} are respectively the parameters XPD_{HV} and XPD_{VH} converted in natural value.

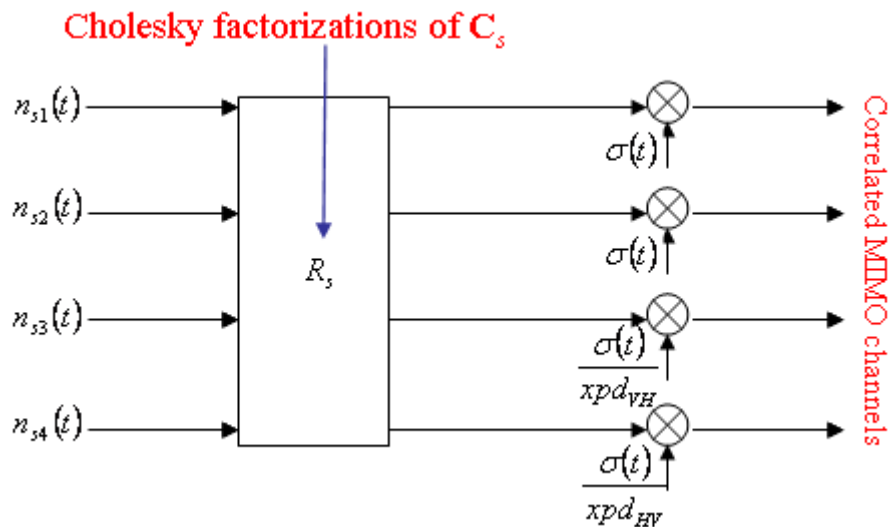


Figure 11: Principle of the MIMO model for terrestrial links in the hybrid channel software

In the current version of the hybrid channel software, C_s is the identity matrix, but this parameter can be easily tuned if correlation matrices are available for dual polarized terrestrial links.

4.3.2 LMS SISO & MIMO physical-statistical model for Tree Shadowed environments

A physical-statistical model developed under a Post-Doctoral grant cofunded by CNES, Thalès Alenia Space France, ONERA and University of Vigo is available in the framework of ENGINES activity. Physical-statistical means that:

- It relies partly on physical bases requiring to some extent a deterministic description of the mobile terminal environment. This physical part enables to reproduce what could be measured in a specific real environment until a given scale of propagation effect. It also offers the possibility to carry out parametric analyses (satellite constellation, link frequency, diversity techniques) on a given specific scenery.
- It relies partly on some statistical models which makes it not fully deterministic. This statistical part enables to decrease the model complexity and its computation time.

The current version of the model concerns only tree shadowed environments. The SISO propagation channel model has been validated using in particular S-band (2.2 GHz) experimental data measured by CNES in Gaillac region. The measurement subsets selected for validation purpose contained mainly roadside plane trees sceneries.

MIMO (dual circular polarization) and SIMO (Rx antenna diversity) extensions have also been developed and included to the final Matlab software. The SISO model and MIMO extension are presented in the following of this section.

4.3.2.1 SISO physical model

This SISO generative model described in [6] basically relies on the multiple scattering theory through a single tree. This electromagnetic approach enables to compute quite rapidly:

- the coherent scattered power and the specific attenuation through a single tree (effects influencing the Rx-Tx direct path)
- the incoherent scattered power or equivalently the diffuse component of the propagation channel due to multipath in the tree canopy.

Its principle is to describe a single tree as a “statistical” tree whose general shape is deterministic but whose canopy description is statistical: only the density inside the canopy of a limited number of branches categories and of leaves is required. For example, these characteristics have been published in [7] for a typical European tree (oak tree) and are shown on Table 6.

Type	Radius (cm)	Length/thickness (cm)	Number density (m3)
Branch (1)	11.4	131	0.013
Branch (2)	6.0	99	0.073
Branch (3)	2.8	82	0.41
Branch (4)	0.7	54	5.1
Branch (5)	0.2	12	56
Leaf	3.7	0.02	420

Table 6: Oak tree canopy geometric description

The relative permittivity of branches and leaves are also required at the selected link frequency. **For frequencies close to 2 GHz**, values published in [7] can be used:

- all branches: $\varepsilon_l = 28 - 7j$
- leaves: $\varepsilon_l = 31 - 8j$.

From these geometric and electromagnetic characteristics of tree canopy, two intermediate electromagnetic parameters are computed by the physical model: the mean scattering amplitude of branches and leaves and the equivalent scattering cross-section per unit volume of the canopy. These intermediate parameters are then combined to the tree canopy geometry (regular or irregular shape) to compute the coherent scattered power, the specific attenuation and the incoherent scattered power **for the user-defined link elevation angle**. If several geometry of trees are included in the scenery, only this last step has to be reproduced for each of them (the intermediate scattering parameters do not change).

Consequently, at S-band and assuming that the tree whose parameters are given on Table 6 is typical enough, the only input parameters that have to be indicated by the model user are the canopies geometry (heights, shapes and dimensions).

The current version of the Matlab software already includes several canopy shapes (see Figure 12):

- regular cylinder (a)
- irregular cylinder (b)
- regular cube (c)
- irregular cube (d)

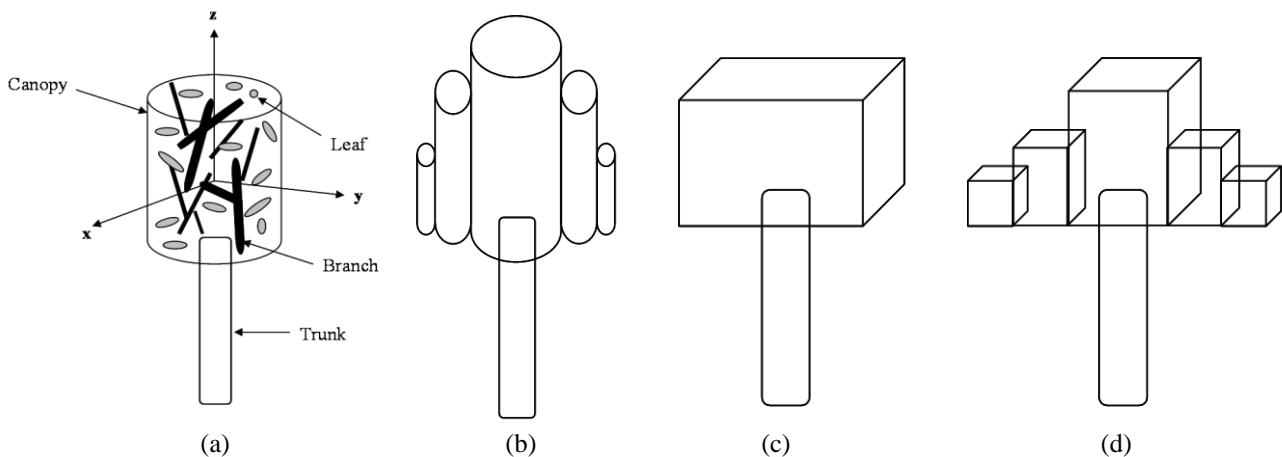


Figure 12: Canopy shapes included in the physical-statistical software

The trunk attenuation is computed using a simplified multiple scattering model since it can be considered as a given branch with a specific orientation.

In the current version of the physical-statistical model, an automatic scenery construction is possible with two levels of input parameters (see Figure 13):

- 1st level mode:
 - Canopy shape (within the 4 possibilities shown on Figure 12)
 - r_C : Radius of the canopies (identical for all trees)
 - Number of roadside trees
 - d_{bT} : Distance between tree canopies (one single value for the whole scenery)
- 2nd level mode (if default values must be modified):
 - r_T : Trunk radius (default value = 0.5 m)
 - h_T : Trunk height (default value = 10 m)
 - h_C : Canopy height (default value = 10 m)
 - h_{Rx} : Rx height (default value = 2 m)
 - w_S : Street width (default value = 10 m)
 - d_{S2T} : Distance from the street to trees (default value = 3 m)

As shown on Figure 13, this automatic scenery consists on two trees alleys on each side of the street. The tree alley that is not crossed by the direct path between the satellite and the mobile terminal ("side 2" in the following) just contributes in terms of multipath incoherent power to the full propagation channel.

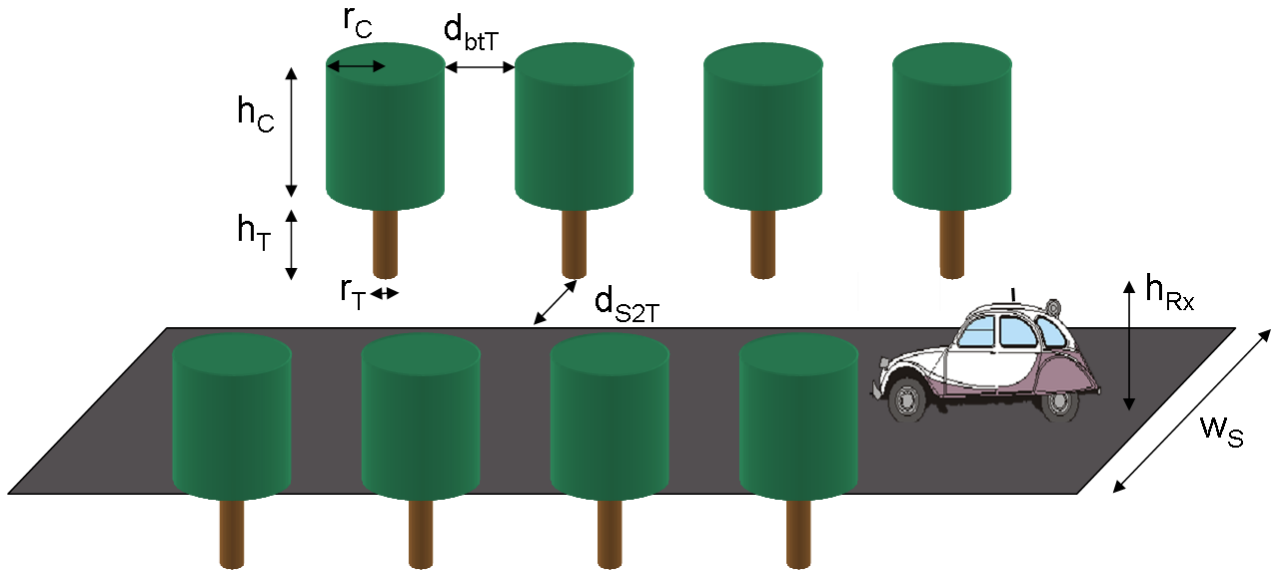


Figure 13: Automatic scenery characteristics

For expert users, it is possible to define a more complex tree shadowed environment. Nevertheless, such a simple configuration quite well reproduces measurement results from CNES S-band experiment in Gaillac (regularly spaced plane trees in the French countryside) as shown in [6].

In the scenery, each tree is a “statistical” tree characterised by canopy parameters such as the ones appearing in Table 6.

Once the physical scenery is built, the electromagnetic computation is performed to get the propagation channel complex envelope spatial/time series $h(t)$:

$$h(t) = \sum_{m=1}^{S_1} \sum_{n=1}^N A_{\text{diff1},mn}(t) \frac{\exp\{j(\phi_{mn} + kd_{mn}(t))\}}{d_{mn}(t)} + A_{d,m}(t) \frac{\exp\{j(\phi_m + kd_m(t))\}}{d_m(t)} \\ + \sum_{w=1}^{S_2} \sum_{n=1}^N A_{\text{diff2},wn}(t) \frac{\exp\{j(\phi_{wn} + kd_{wn}(t))\}}{d_{wn}(t)}$$

where

$A_{\text{diff1},mn}(t)$ is the diffuse multipath complex envelope from the n^{th} point scatterer of the canopy of the m^{th} tree on side 1 of the street.

N is an internal parameter of the model equal to the total number of scatterers in a single tree

S_1 is the number of tree on side 1 of the road.

$A_{d,m}(t)$ is the direct path complex envelope from the m^{th} tree on side 1 of the street.

$A_{\text{diff2},mn}(t)$ is the diffuse multipath complex envelope from the n^{th} scatterer of the m^{th} tree on side 2 of the street.

S_2 is the number of tree on side 2 of the road.

The impact of the antenna pattern on these channel components is roughly taken into account by the physical-statistical model.

To decrease the simulation time and to enable statistical analyses from a single specific scenery, a stochastic model has been derived from this first physical one as shown on Figure 14:

- $\sigma(t)$ is the diffuse multipath power directly inferred from the diffuse multipath complex envelope computed by the physical model. It multiplies a complex white Gaussian noise whose Doppler spectrum is computed using the Aulin's model [8] ("Doppler filter" on Figure 14).
- $\sigma_q(t)$ is the local standard deviation of the direct path power, inferred from direct path complex envelope computed by the physical model. It multiplies a real Gaussian noise filtered by a 1st order low-pass filter ("Shadowing filter" on Figure 14) characterised by a correlation distance equal to 1 m.
- $q(t)$ is the local mean of the direct path power, inferred from direct path complex envelope computed by the physical model.
- $\exp(j\phi)$ is the Doppler shift due to the mobile terminal motion
- $v(t)$ is a multiplicative temporal variability of the propagation channel caused by trees swaying due to wind. Even when the terminal is static (nomadic case), this component involves propagation channel fluctuations. To compute this channel component, a stochastic model of wind was developed and combined with a "masses attached to spring" representation of tree canopies (see [6] for details). Consequently, this standalone model provides time varying channel contribution from a single input parameter to be indicated by the software user: the average wind speed, w_m .

This model still relies on physical bases with a user-defined scenery but also introduces a stochastic behaviour suitable for classical air interface assessments.

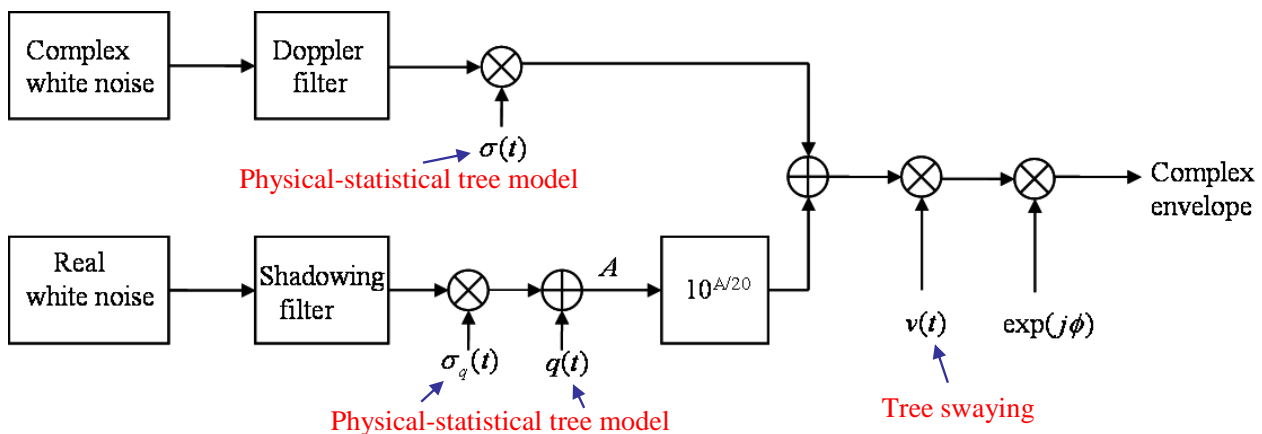


Figure 14: Roadside trees stochastic model relying on physical bases

Model implementation:

The SISO physical-statistical model is implemented under Matlab. The software generates output files containing propagation channel spatial series (channel complex envelope). Consequently, specific dumps must be synthesised before to be read within global air interface simulators.

4.3.2.2 MIMO extension

The SISO physical-statistical model has been extended into a 2x2 MIMO model described in [8]. This MIMO model is suitable to address dual circular polarized (RHCP and LHCP) diversity in a Land Mobile Satellite link at S-band. This MIMO extension is strictly stochastic to get reasonable computation times, even if it could have been possible to use the physical approach to generate MIMO channel time/spatial series. Stochastic means that it relies on the use of two correlation matrices:

- C_s for the small scale fading (diffuse multipath component of the propagation channel)
- C_l for the large scale fading (direct path component of the propagation channel).

Using these correlation matrices, the SISO model presented in the previous section is extended into a MIMO one generating 4 correlated propagation channel complex envelopes according to the description shown on Figure 15.

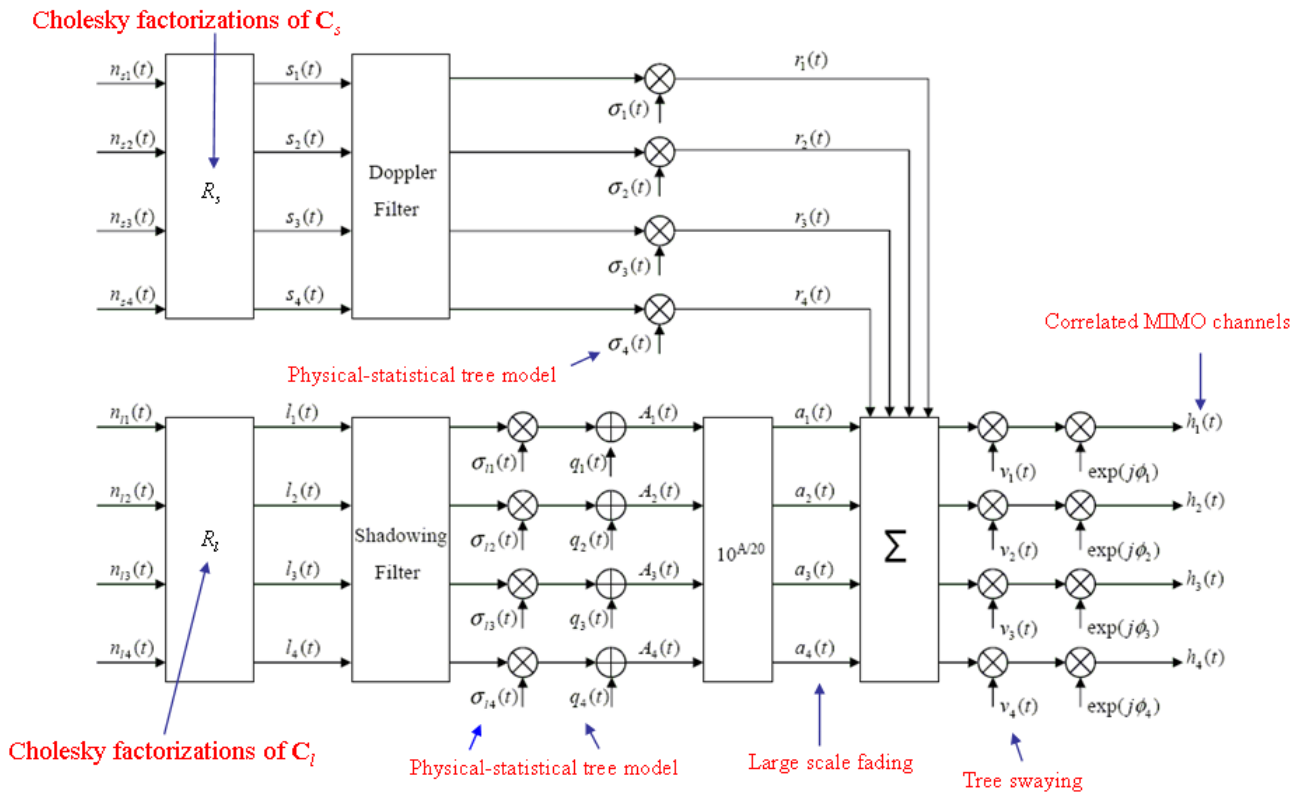


Figure 15: 2x2 MIMO Roadside trees stochastic model relying on physical bases

In the current version of the model, C_s is assumed to be the identity matrix because existing measurements on slant path at S-band exhibits quite low correlation between the 4 MIMO channels in roadside trees environment [10]:

	R/R	L/L	R/L	L/R
R/R	1	0.03	0.02	0.09
L/L	0.03	1	0.12	0.01
R/L	0.02	0.12	1	0.01
L/R	0.09	0.01	0.01	1

Table 7: Small scale fading MIMO correlation matrix given in [10] for roadside trees environment

Nevertheless, it is also possible to include such a measured small scale fading correlation matrix.

For the large scale fading correlation, due to the lack of experimental data, a FDTD (Finite Difference Time Difference) model has been run to characterize C_l for the canonical case of a single deterministic tree (see [9] for details). The resulting C_l matrix is shown on Table 8. This correlation matrix is pretty close to the one assessed from slant path S-band measurements and presented in [10].

TR 3.1

	R/R	L/L	R/L	L/R
R/R	1	0.87	0.30	0.43
L/L	0.87	1	0.26	0.47
R/L	0.30	0.26	1	0.49
L/R	0.43	0.47	0.49	1

Table 8: Large scale fading MIMO correlation matrix assessed from FDTD simulations

An example of 2x2 MIMO channel fading series is shown on Figure 16.

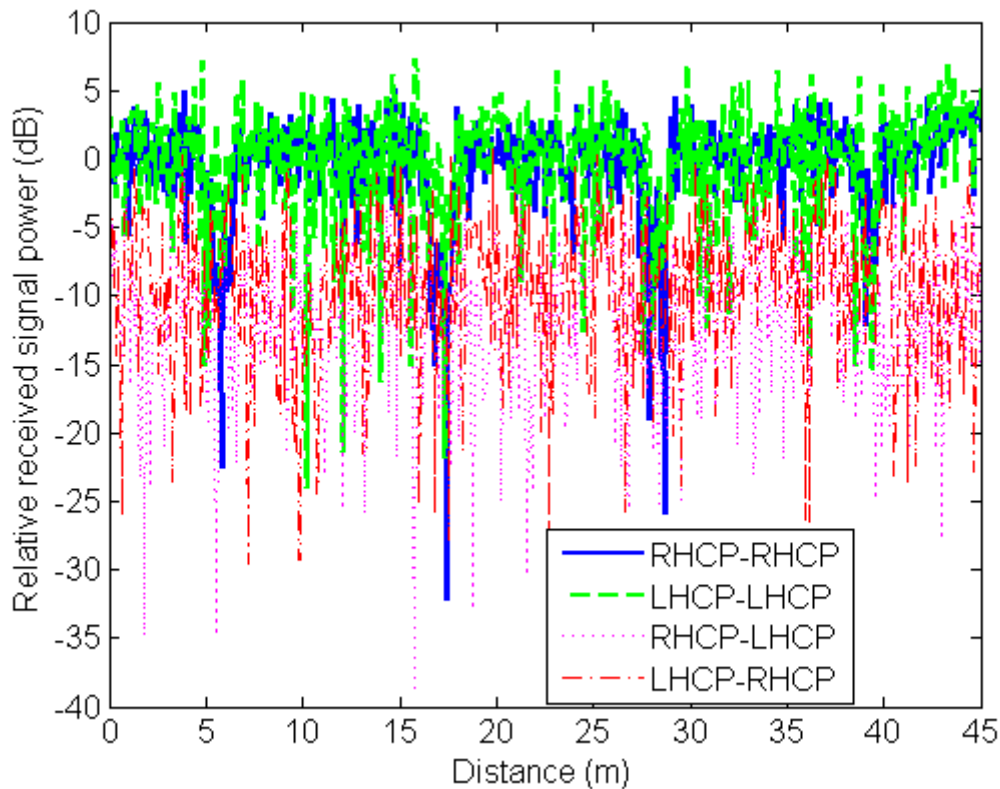


Figure 16: Example of 2x2 MIMO spatial series synthesised using the roadside trees model at S-band

Model implementation:

The MIMO physical-statistical model is implemented under Matlab. The software generates output files containing propagation channel spatial series (channel complex envelope). Consequently, specific dumps must be synthesised before to be read within global air interface simulators.

4.3.2.3 Reference parameterization

As mentioned in section 4.3.2.1, the SISO physical-statistical channel model has been validated using S-band measurement datasets from CNES experiment in the French countryside. This validation required to fit the scenery description on the real one (typical plane trees regularly spaced out by 9 m). From this parameters set used for validation purpose, a reference configuration have been inferred and it is suggested to consider it as a typical reference application case (see Table 9). The SISO parameters is completed with MIMO parameters published in [9].

Obviously, the interest of such a physical model is to be able to address in particular various realistic roadside trees sceneries. Consequently, it can be used beyond the suggested reference parameterization, in particular when the description of real environments is available.

Input parameter	Reference value
Link frequency	S-band (2 GHz in [6])
Link elevation angle	30°
Canopy shape	cylindrical, regular
Radius of the canopies (r_C)	2.5 m
Distance between tree canopies (d_{btT})	4 m
Height of the canopy (h_C)	20 m
Street width (w_S)	6.5 m
Average wind speed (w_m)	3 m/s
Other SISO model parameters	Default values
Small scale fading correlation matrix (C_s)	“Ideal” case: Identity matrix or “Real” case: $\begin{pmatrix} 1 & 0.03 & 0.02 & 0.09 \\ 0.03 & 1 & 0.12 & 0.01 \\ 0.02 & 0.12 & 1 & 0.01 \\ 0.09 & 0.01 & 0.01 & 1 \end{pmatrix}$
Large scale fading correlation matrix (C_l)	$\begin{pmatrix} 1 & 0.87 & 0.30 & 0.43 \\ 0.87 & 1 & 0.26 & 0.47 \\ 0.30 & 0.26 & 1 & 0.49 \\ 0.43 & 0.47 & 0.49 & 1 \end{pmatrix}$

Table 9: Reference set of input parameters for the physical-statistical roadside trees model

Suggested terminal speed are similar to the one proposed within DVB-SH working group: 3 km/s, 50 km/h and 120 km/h.

4.3.3 LMS SISO & MIMO empirical models

4.3.3.1 SISO empirical models

Three S-band SISO empirical models are currently available and implemented into various softwares:

- the Perez-Fontan 3-state model: A DLL implementation of the model has been made available by CNES within the DVB-SH and DVB-NGH working groups
- the ESA enhanced 2-state model: An executable implementation of the model has been made available by ESA within the DVB-NGH working group
- the CNES enhanced 2-state model: A DLL implementation of the model is available and could be used as an equivalent alternative to the ESA model for activities out of DVB-NGH

These models are presented in the following of the section, and some suggestions are made concerning their use, depending on the activity framework.

4.3.3.1.1 3-state model (DVB-SH)

This model detailed in [11] and [12] has been widely used since the 90's. It is fully empirical (or equivalently statistical) and relies on a specific S-band measurements dataset including various environments (open, intermediate tree shadow, heavy tree shadow, suburban, urban). Basically, its principle is to share the LMS propagation channel into 3 shadowing states:

- State 1: "LOS"
- State 2: "Shadowing" (for example typically isolated trees in suburban areas)
- State 3: "Heavy Shadowing/Blockage" (for example typically houses in suburban areas).

In the generative model, the state change (large scale) is synthesised using a 3-state Markov chain model whose input parameters are the initial state vector and the transition matrix. Two more input parameters have also been added:

- Each state is assumed to have a minimum length ("state length")
- A transition between two states happens over a given transition distance ("state transition length").

Then, inside each state (mid-scale), the channel fading is assumed to follow a Loo distribution (basically the distribution of a Rice process whose direct path amplitude is log-normally distributed). The input parameters for each state are the log-normal parameters of the direct path amplitude and the multipath power assumed to be constant. Another input parameter at this intermediate scale is the shadowing correlation length that influences the dynamics of the direct path amplitude change within one state.

At small scale, in the CNES implementation provided to DVB-SH, the fading dynamics is taken into account by using a Zheng-Xiao model (Classical Doppler spectrum) [5]. Moreover, the Doppler shift affecting the direct path normalised by the maximum multipath Doppler shift must also be indicated.

To summarize, the 3-state model input parameters are the following:

- Initial state vector : $[W]$
- Transition matrix : $[P]$
- Correlation distance of the shadowing : d_{corr}
- Lognormal parameters (for each state) : α and ψ
- Diffuse component power (for each state) : MP
- Frame length (minimum state length) : L_{frame}
- State Transition length : L_{trans}
- Doppler shift of the satellite direct path (normalized to maximum Doppler) : $f_{d,\text{direct}}$

For the model provided to both the DVB-SH and DVB-NGH working groups the input parameters values inferred from [11] and [12] are shown on Table 10.

For a GEO satellite, a suggested default value for $f_{d,\text{direct}}$ is 0.7.

Model implementation:

The 3-state Markov model is implemented as a Dynamic Link Library (DLL) in particular to be compatible of various software languages. Moreover, the software generates propagation channel sample after sample meaning that it can be run continuously over very long simulation time and does not induce any writing (and then reading in simulator) of output files. Consequently, it can be included as a module within global air interface simulators.

Environment	State 1			State 2: Shadowing			State 3: Blockage		
	α (dB)	ψ (dB)	MP (dB)	α (dB)	ψ (dB)	MP (dB)	α (dB)	ψ (dB)	MP (dB)
Open	0.1	0.37	-22.0	-1.0	0.5	-22.0	-2.25	0.13	-21.2
Suburban	-1.0	0.5	-13.0	-3.7	0.98	-12.2	-15.0	5.9	-13.0
Intermediate Tree-Shadow	-0.4	1.5	-13.2	-8.2	3.9	-12.7	-17.0	3.14	-10.0
Heavy Tree-Shadow	-	-	-	-10.1	2.25	-10.0	-19.0	4.0	-10.0

Environment	[P]			[W]	d_{corr} (m)	L_{frame} (m)	L_{trans} (m)
Open	0.9530	0.0431	0.0039	0.5	2.5	8.9	12.4
	0.0515	0.9347	0.0138	0.375		7.5	
	0.0334	0.0238	0.9428	0.125		4.0*	
Suburban	0.8177	0.1715	0.0108	0.4545	1.7	5.2	2.2
	0.1544	0.7997	0.0459	0.4545		3.7	
	0.1400	0.1433	0.7167	0.091		3.0*	
Intermediate Tree-Shadow	0.7193	0.1865	0.0942	0.3929	1.5	6.3	2.6
	0.1848	0.7269	0.0883	0.3571		6.3	
	0.1771	0.0971	0.7258	0.25		4.5	
Heavy Tree-Shadow	0.7792	0.0452	0.1756	0	1.7	-	3.5
	0	0.9259	0.0741	0.5		4.8	
	0	0.0741	0.9259	0.5		4.5	

* These values have been extrapolated since they are not given in [11] or [12].

Table 10: 3-state model input parameters at S-band for a 40° elevation angle (top: Loo distributions parameters, bottom other input parameters)

4.3.3.1.2 ESA enhanced 2-state model (DVB-NGH)

This quite recent empirical model presented in [13] relies on the same S-band experimental dataset as the one used to develop the 3-state channel model in the 90's. Its analytical framework can be considered as a generalization of the multi-state concept used in the 3-state Markov model since for each of its 2-state (state 1 or "GOOD" and state 2 or "BAD"), the Loo distribution parameters are randomly drawn into empirical distributions. Another novelty when compared with the 3-state model is to introduce both a Markov chain option and a semi-Markov chain option. Indeed, Markov chain models seem to be a little bit less realistic than semi-Markov ones in terms of second order statistics (in particular average fade duration) when compared with experimental data [13].

The detailed principle of the model is the following:

- At large scale, the change between BAD and GOOD states is synthesised using a Markov chain with input transition matrix [P] or a semi-Markov chain with a lognormal distribution (input parameters: $\{m_{dur,k}, \sigma_{dur,k}\}_{k \in [1;2]}$, k being the state index)
- Within state k ($k \in [1;2]$), the Loo parameters (α_k, ψ_k, MP_k) or equivalently ($M_{A,k}, \Sigma_{A,k}, MP_{,k}$) are randomly drawn as follows:
 - Random draw of Loo parameter $M_{A,k}$ in a Gaussian distribution with input parameters $(\mu_{1,k}, \sigma_{1,k})$

TR 3.1

- Random draw of Loo parameter $\Sigma_{A,k}$ in a Gaussian distribution with input parameters $(\mu_{2,k}, \sigma_{2,k})$ conditioned by the $M_{A,k}$ value:

$$\begin{cases} \mu_{2,k} = a_{1,k} \times M_{A,k}^2 + a_{2,k} \times M_{A,k} + a_{3,k} \\ \sigma_{2,k} = b_{1,k} \times M_{A,k}^2 + b_{2,k} \times M_{A,k} + b_{3,k} \end{cases}$$

- Random draw of Loo parameter MP in a Gaussian distribution with input parameters $(\mu_{3,k}, \sigma_{3,k})$

The direct path amplitude short term fluctuations within one state is generated using a correlation length L_{corr} equal to 1 m at S-band.

- The small scale fading dynamics is taken into account using a Butterworth Doppler filter defined as follows:

$$|H_{butt}(f)|^2 = \frac{B}{1 + (f/f_c)^{2k}}$$

where the Butterworth filter is implemented such as it presents a maximum ripple of 3 dBs up to $0.9 \times v_m/\lambda$, and an attenuation of 100 dBs at $3 \times v_m/\lambda$, v_m being the terminal speed.

This Doppler spectrum shaping seems to have been selected quite subjectively (see [13]).

- Additional modelling elements:
 - To avoid sharp changes other than those due to multipath, a maximum shadowing/blockage slope of 5dB/m is allowed. If larger values are generated, a linear interpolation state transition for the shadowing is included.
 - For the Markov chain model, the minimum state length, L_{frame} , is said to be equal to 5 m.

Suggested input parameters values are detailed in Table 11. They correspond to values published in [13] which were inferred from the same S-band measurements as the ones used to develop the 3-state Markov model.

Model implementation:

The ESA enhanced 2-state SISO model (Markov chain model only) is probably included within the MIMO_LMS executable [14] provided by ESA to the DVB-NGH working group. Indeed, even if it is said that it is the 3-state model which is included in MIMO_LMS according to document [15], this same reference document refers to [16] where only the 2-state model is mentioned to generate SISO reference channel.. The software generates output files containing propagation channel spatial series (channel complex envelope). Consequently, specific dumps must be synthesised before to be read within global air interface simulators.

Input parameter	Open rural	Intermediate tree shadowed	Heavy tree shadowed	Suburban	Urban
[P]	$\begin{bmatrix} [0.93][0.07] \\ [0.02][0.98] \end{bmatrix}$	$\begin{bmatrix} [0.6] [0.4] \\ [0.19][0.81] \end{bmatrix}$	$\begin{bmatrix} [0.75][0.25] \\ [0.18][0.82] \end{bmatrix}$	$\begin{bmatrix} [0.91][0.09] \\ [0.12][0.88] \end{bmatrix}$	$\begin{bmatrix} [0.92][0.08] \\ [0.08][0.92] \end{bmatrix}$
$m_{dur,1}$ (m)	27.2	20.7	22.4	27.7	26.5
$\sigma_{dur,1}$ (m)	6.2	4.8	7.7	10.6	10.4
$m_{dur,2}$ (m)	23.0	26.8	25.4	26.0	30.9
$\sigma_{dur,2}$ (m)	7.2	3.8	7.8	9.8	9.0

Input parameter	Open rural	Intermediate tree shadowed	Heavy tree shadowed	Suburban	Urban
$\mu_{1,1}$	0.2237	-0.3534	-4.0557	-2.3553	0.0586
$\sigma_{1,1}$	0.2111	0.2198	1.0843	0.9962	0.6404
$\mu_{1,2}$	-0.9379	-9.6427	-8.2585	-6.3961	-9.7143
$\sigma_{1,2}$	1.0087	2.4876	1.0004	2.5466	7.2610
$a_{1,1}$	0.3246	0.1366	-0.0127	-0.0522	0.2837
$a_{2,1}$	0.1419	-0.0754	0.0104	0.0569	0.0905
$a_{3,1}$	0.1262	0.3631	2.6821	1.7999	0.4704
$a_{1,2}$	-0.1131	-0.0302	0.1006	0.0076	-0.0024
$a_{2,2}$	-0.845	-0.5337	1.5844	-0.3422	-0.2411
$a_{3,2}$	-0.1786	0.7417	9.3947	-0.3842	0.5636
$b_{1,1}$	0.1038	-0.7478	0.0337	-0.0046	-0.0638
$b_{2,1}$	-0.1173	-0.6613	0.2136	-0.0865	0.0044
$b_{3,1}$	0.0391	-0.0615	0.699	0.0401	0.0473
$b_{1,2}$	-0.007	0.0337	0.0924	0.0335	0.018
$b_{2,2}$	-0.1288	0.4363	1.5971	0.729	0.196
$b_{3,2}$	-0.0342	1.613	7.3515	4.006	0.7561
$\mu_{3,1}$	-27.3077	-14.1667	-12.2083	-23.3438	-15.7778
$\sigma_{3,1}$	2.2871	1.6422	3.3003	5.5742	4.4096
$\mu_{3,2}$	-27.7143	-14.3846	-12.8542	-24.6129	-16.8571
$\sigma_{3,2}$	3.0742	1.6093	2.1536	5.7889	8.9336

Table 11: ESA enhanced 2-state model input parameters at S-band for a 40° elevation angle (top: Markov/semi-Markov chain parameters, bottom: Loo distribution related parameters)

4.3.3.1.3 CNES enhanced 2-state model

This empirical model has been derived from CNES S-band measurement datasets measured in Gaillac and Auch between 2006 and 2008 in various environments. Its basic analytical framework is very similar to the ESA enhanced 2-state model. Nevertheless, to fit CNES experimental data characteristics, slight modifications have been brought to the model described in [13]. These differences between CNES and ESA models are detailed in Table 12.

ESA model	CNES model
Gaussian distribution of the direct path amplitude standard deviation per event conditioned to the event mean value	Linear relation between the standard deviation of direct path amplitude and its mean value per event
Gaussian distribution of the Rice factor mean value per event	Linear relation between the Rice factor mean value and the direct path amplitude mean value per event
Transition slopes : maximum value inferred from the experimental data	Transition Slopes: linear relation between the slope and the shadowing step between both states

Table 12: Differences between ESA and CNES enhanced 2-state models

The description of input parameters for the CNES 2-state Markov and semi-Markov models is summarized in Table 8.

Model type	Parameter	Description
2-state Markov chain only	$[W] = \begin{bmatrix} P_1 \\ P_2 \end{bmatrix}$	State probabilities
	$[P] = \begin{bmatrix} P_{11} & P_{12} \\ P_{21} & P_{22} \end{bmatrix}$	State transition probabilities
	L_{Frame}	Frame length (min. state length) set to 1 m
2-state semi-Markov chain only	$(m_{\text{dur}}, \sigma_{\text{dur}})_{1,2}$	Mean and standard deviation of the log-normal law assumed for events duration
Common to both models	$(M_A, \Sigma_A)_{1,2}$	Parameters of the $\langle A \rangle$ distribution, ($\langle A \rangle$ is the average value of the direct path amplitude A (one set for each state, in dB))
	$\text{std}(A_{1,2}) = g_{1,2}(\langle A_{1,2} \rangle)$	Linear function linking the $\langle A \rangle$ value to the standard deviation of A (one set for each state)
	$\langle K_{1,2} \rangle = h_{1,2}(\langle A_{1,2} \rangle)$	Linear function linking $\langle A \rangle$ and $\langle K \rangle$ (possibly one set for each state)
	$L_{\text{corr}1,2}$	Correlation lengths of the states 1 and 2 (in meters)
	$S_p = f(\Delta A)$	Linear function linking the transition slope and ΔA (difference between A before and after the transition)

Table 13: CNES enhanced 2-state models input parameters

Moreover, in the current version of the CNES model, the small scale fading dynamics is taken into account by using a Zheng-Xiao model (Classical Doppler spectrum) [5]. An activity is on-going to infer more realistic Doppler spectra from CNES measurements.

Suggested input parameters values are detailed in Table 14. They are suitable for a link to a GEO satellite at S-band. The different environment were measured during the following experiments:

- Gaillac 2006 (see §4.3.2.1 for details, elevation angle between 25 and 50°): Tree alley environment
- Auch 2007 (2.2 GHz, elevation angle equal to 35°, same set-up as the one presented in [4]): Town to town environment (road in the French countryside including small villages between two medium-size cities)
- Auch 2008 (see experiment details in [4]): Wooded, Suburban and Urban environment

Environment	Wooded	Suburban	Urban	Town to town	Tree alley
[P]	$\begin{bmatrix} [0.97][0.03] \\ [0.03][0.97] \end{bmatrix}$	$\begin{bmatrix} [0.99][0.01] \\ [0.03][0.97] \end{bmatrix}$	$\begin{bmatrix} [0.98][0.02] \\ [0.03][0.97] \end{bmatrix}$	$\begin{bmatrix} [0.99][0.01] \\ [0.02][0.98] \end{bmatrix}$	$\begin{bmatrix} [0.96][0.04] \\ [0.09][0.91] \end{bmatrix}$
[W]	$\begin{bmatrix} [0.45] \\ [0.55] \end{bmatrix}$	$\begin{bmatrix} [0.80] \\ [0.20] \end{bmatrix}$	$\begin{bmatrix} [0.62] \\ [0.38] \end{bmatrix}$	$\begin{bmatrix} [0.61] \\ [0.39] \end{bmatrix}$	$\begin{bmatrix} [0.68] \\ [0.32] \end{bmatrix}$
m_1	2.86	3.94	N/A	3.13	2.05
σ_1	0.98	1.18	N/A	1.36	1.81
m_2	2.54	2.90	2.97	2.14	0.54
σ_2	1.68	1.17	1.17	1.89	1.71

Environment	Wooded	Suburban	Urban	Town to town	Tree alley
$M_{A,1}$	-5.70	-6.16	-5.30	-6.62	-5.64
$\Sigma_{A,1}$	2.11	1.38	1.62	2.16	0.9
$M_{A,2}$	-12.20	-14.74	-15.86	-14.33	-8.27
$\Sigma_{A,2}$	1.33	0.97	2.25	2.54	1.26
g_1	$0.14\langle A \rangle + 2.85$	$0.20\langle A \rangle + 3.17$	$0.13\langle A \rangle + 3.29$	$0.08\langle A \rangle + 2.49$	$0.27\langle A \rangle + 2.4$
g_2	$-0.08\langle A \rangle + 1.70$	$-0.23\langle A \rangle - 0.35$	$-0.08\langle A \rangle + 2.13$	$-0.11\langle A \rangle + 1.12$	$-0.43\langle A \rangle - 2.47$
h_1	$0.66\langle A \rangle + 9.61$	$0.96\langle A \rangle + 13.16$	$1.01\langle A \rangle + 10.61$	$0.66\langle A \rangle + 16.17$	$0.72\langle A \rangle + 15.40$
h_2	$0.71\langle A \rangle + 7.66$	$0.61\langle A \rangle + 10.52$	$0.44\langle A \rangle + 5.67$	$0.71\langle A \rangle + 14.51$	$1.29\langle A \rangle + 18.67$
L_{corr1}	1.50	2.83	1.82	2.47	1.21
L_{corr2}	0.01	0.01	0.04	1.25	0.42
f	$0.43\Delta A + 3.24$	$0.43\Delta A + 3.24$	$0.94\Delta A + 5.24$	$0.57\Delta A + 3.21$	$0.77\Delta A + 3.61$

Table 14: CNES enhanced 2-state model input parameters at S-band for a GEO satellite
(top: Markov/semi-Markov chain parameters, bottom: other input parameters)

Model implementation:

The CNES 2-state model is implemented as a Dynamic Link Library (DLL) with the same interface as the 3-state Markov model provided to DVB-SH and DVB-NGH working groups.

4.3.3.1.4 Comparative analysis of SISO empirical channel models

All the 3 empirical SISO models presented in previous sections might be available for ENGINES partners contributing to DVB-NGH activity. Nevertheless, some limitations and constraints must be identified.

	Pros	Cons
3-state Markov model	<ul style="list-style-type: none"> ○ Model extensively used during the last 2 decades and recently as a reference channel of the DVB-SH working group ○ Variety of environments ○ DLL implementation that enables its integration within global air interface simulators ○ Available for partners carrying out activity in the framework of DVB-SH, DVB-NGH and ENGINES ○ Compatible with the MIMO extension described in §4.3.3.2 ○ Possibility to consider time-varying Rx speed if required ○ CNES implementation so possibility to tune input parameters (from other experiment or to solve LOS calibration problems for example) 	<ul style="list-style-type: none"> ○ Defaults of experimental datasets from which input parameters have been inferred: <ul style="list-style-type: none"> ○ limited datasets: in suburban environment for example, the original spatial series probably corresponds to a travelled distance less than 300 m ○ quality: the LOS calibration performed before developing this model probably suffered from a lack of helpful parameters monitoring (see TR4.1 technical report) ○ quite poor knowledge of real environment measurements ○ 1st and second order characteristics validation have shown that enhanced 2-state models should be more quite more realistic (see [13])
ESA 2-state model(s)	<ul style="list-style-type: none"> ○ Model quite new but proposed to and accepted by DVB-NGH working group ○ Model published in reference journal ○ Variety of environments ○ Compatible with the MIMO extension described in §4.3.3.2 (it is already included within the MIMO model accepted by the DVB-NGH working group [16]) ○ Better performances in terms of 1st and 2nd order statistics than the 3-state Markov model 	<ul style="list-style-type: none"> ○ Currently available for partners carrying out activity in the framework of DVB-NGH <u>only</u> ○ Same defaults as the 3-state model concerning the original measurements since they are similar ○ Executable software implementation: <ul style="list-style-type: none"> ○ Requires an “off-line” synthesis of propagation channel time series (which can be problematic for large simulations) ○ The current software seems not to guarantee the input sampling time or simulation time according to first tests (To be confirmed, bug to be solved by ESA if required ?) ○ Input terminal speed is constant ○ Not implemented by an ENGINES partner so no possibility to tune the input parameters unless upon request to ESA ○ Only the Markov model seems included in the ESA implemented software whereas semi-Markov approach has been shown to perform better

CNES 2-state models	<ul style="list-style-type: none"> ○ <u>Large</u> variety of environments ○ Compatible with the MIMO extension described in §4.3.3.2 ○ DLL implementation that enables its integration within global air interface simulators (same interface as 3-state model so compatible with the same existing air interface simulators) ○ Possibility to consider time-varying Rx speed if required ○ CNES implementation so possibility to tune input parameters (from other experiment or to solve LOS calibration problems for example) ○ Good knowledge of experimental environments and measurement routes. In particular, distances large enough to be representative of larger distances ○ Available for partners carrying out activity in the framework of ENGINES ○ Both the Markov and the semi-Markov approaches are included in the DLL software. Semi_Markov model should be preferred when possible. 	<ul style="list-style-type: none"> ○ Model quite new, not proposed to any standardization working group ○ Model not published in a reference journal (should be done quite rapidly) ○ Not compared yet with the 3-state and the ESA 2-state models (should be done quite rapidly)
----------------------------	--	--

Table 15: Comparative analysis of the 3-state, ESA 2-state and CNES 2-state SISO propagation channel softwares

Suggestions of use

- If consistency with past air interface assessments (such as comparison with DVB-SH for example) is required, the 3-state Markov model should be used if new simulations cannot be done for these reference air interfaces.
- For direct contribution to DVB-NGH, the ESA 2-state model must be preferred if the probable current bugs are solved by ESA and if executable software form is not forbidden (typically could be problematic for very large simulations).
- For analyses within ENGINES but not within the framework of DVB-NGH referenced activity, the CNES 2-state semi-Markov model must be preferred.

Suggested terminal speed are similar to the one proposed within DVB-SH working group: 3 km/s, 50 km/h and 120 km/h.

4.3.3.2 MIMO extension

The MIMO_LMS software provided by ESA to DVB-NGH working group implements a MIMO extension of the SISO model presented in §4.3.3.1.2. The principle of such a MIMO model derived from a specific SISO one is described in [16]. It relies on the computation and the use of correlation matrices for both the large scale fading, C_l , and the small scale fading, C_s , similarly to the approach presented in §4.3.2.2. In [16], C_l is inferred from experimental results for open rural, suburban and urban environments (see Table 16). These experimental results were published in [10]. The matrix considered for open rural in [16] must more probably be affected to a tree-lined road scenery (“main road” environment in [10]), so it may also be used at least for the Intermediate Tree Shadowed environment of the SISO model described in §4.3.3.1.2.

Open rural/Intermediate tree shadowed					Suburban					Urban				
	R/R	L/L	R/L	L/R		R/R	L/L	R/L	L/R		R/R	L/L	R/L	L/R
R/R	1	0.86	0.85	0.90	R/R	1	0.76	0.76	0.83	R/R	1	0.86	0.86	0.92
L/L	0.86	1	0.91	0.87	L/L	0.76	1	0.83	0.75	L/L	0.86	1	0.89	0.85
R/L	0.85	0.91	1	0.88	R/L	0.76	0.83	1	0.78	R/L	0.86	0.89	1	0.93
L/R	0.90	0.87	0.88	1	L/R	0.83	0.75	0.78	1	L/R	0.92	0.85	0.93	1

Table 16: Large scale fading correlation matrices for the MIMO empirical model

In [16], C_s is defined as follows:

$$C_s = R_{Tx}^T \otimes R_{Rx}$$

$$\text{with } \begin{cases} R_{Rx} = \begin{pmatrix} 1 & 2\sqrt{(1-\gamma)\gamma}\rho_{Rx} \\ 2\sqrt{(1-\gamma)\gamma}\rho_{Rx} & 1 \end{pmatrix} \\ R_{Tx} = \begin{pmatrix} 1 & 2\sqrt{(1-\gamma)\gamma}\rho_{Tx} \\ 2\sqrt{(1-\gamma)\gamma}\rho_{Tx} & 1 \end{pmatrix} \end{cases} \text{ where } \gamma = \frac{xpc + xpd}{(1+xpc)(1+ xpd)}$$

Where

\otimes denotes the Kronecker product

ρ_{Rx} and ρ_{Tx} are respectively the small scale fading component of the correlation coefficients at Rx and Tx sides

$xpc = 10^{XPC_{env}/10}$, XPC_{env} being the cross polar coupling of the propagation environment

$xpd = 10^{XPD_{ant}/10}$, XPD_{ant} being the cross polar discrimination of antennas

The values of these input parameters of the MIMO model presented in [16] are shown on Table 17. The tree shadowed environments are not addressed in [16].

	Open rural	Suburban	Urban
XPC_{env} (dB)	15	6	5
XPD_{ant} (dB)	15	15	15
ρ_{Rx}	0.5	0.5	0.5
ρ_{Tx}	0.4	0.5	0.5

Table 17: MIMO extension input parameters

From these input parameters, it is possible to derive the small scale correlation matrix, C_l , for these three environments (see Table 18). **This results exhibits quite high correlation coefficients, but due to the current lack of experimental or alternative data for these environments, it is suggested to use them for LMS MIMO simulations.**

Open rural/Intermediate tree shadowed					Suburban					Urban				
	R/R	L/L	R/L	L/R		R/R	L/L	R/L	L/R		R/R	L/L	R/L	L/R
R/R	1	0.24	0.19	0.04	R/R	1	0.41	0.41	0.17	R/R	1	0.44	0.44	0.19
L/L	0.24	1	0.04	0.19	L/L	0.41	1	0.17	0.41	L/L	0.44	1	0.19	0.44
R/L	0.19	0.04	1	0.24	R/L	0.41	0.17	1	0.41	R/L	0.44	0.19	1	0.44
L/R	0.04	0.19	0.24	1	L/R	0.17	0.41	0.41	1	L/R	0.19	0.44	0.44	1

Table 18: Small scale fading correlation matrices for the MIMO empirical model

Then starting from both correlation matrices and the γ and XPD_{ant} parameters, the general principle to extend the SISO channel model into a MIMO one is basically shown on Figure 17. The processes $\{n_{sk}(t)\}_{1 \leq k \leq 4}$ are complex normalised Gaussian processes generated with a specific Doppler spectrum shaping (see SISO models). The processes $\{n_{lk}(t)\}_{1 \leq k \leq 4}$ are real normalised Gaussian processes generated with a 1st order filter characterised by its correlation length (see SISO models). The $\sigma(t)$ process corresponds to the multipath amplitude defined by $MP = 10 \log_{10}(2\sigma^2)$. $M_A(t), \Sigma_A(t)$ are the instantaneous direct path parameters of the Loo distribution (see SISO models).

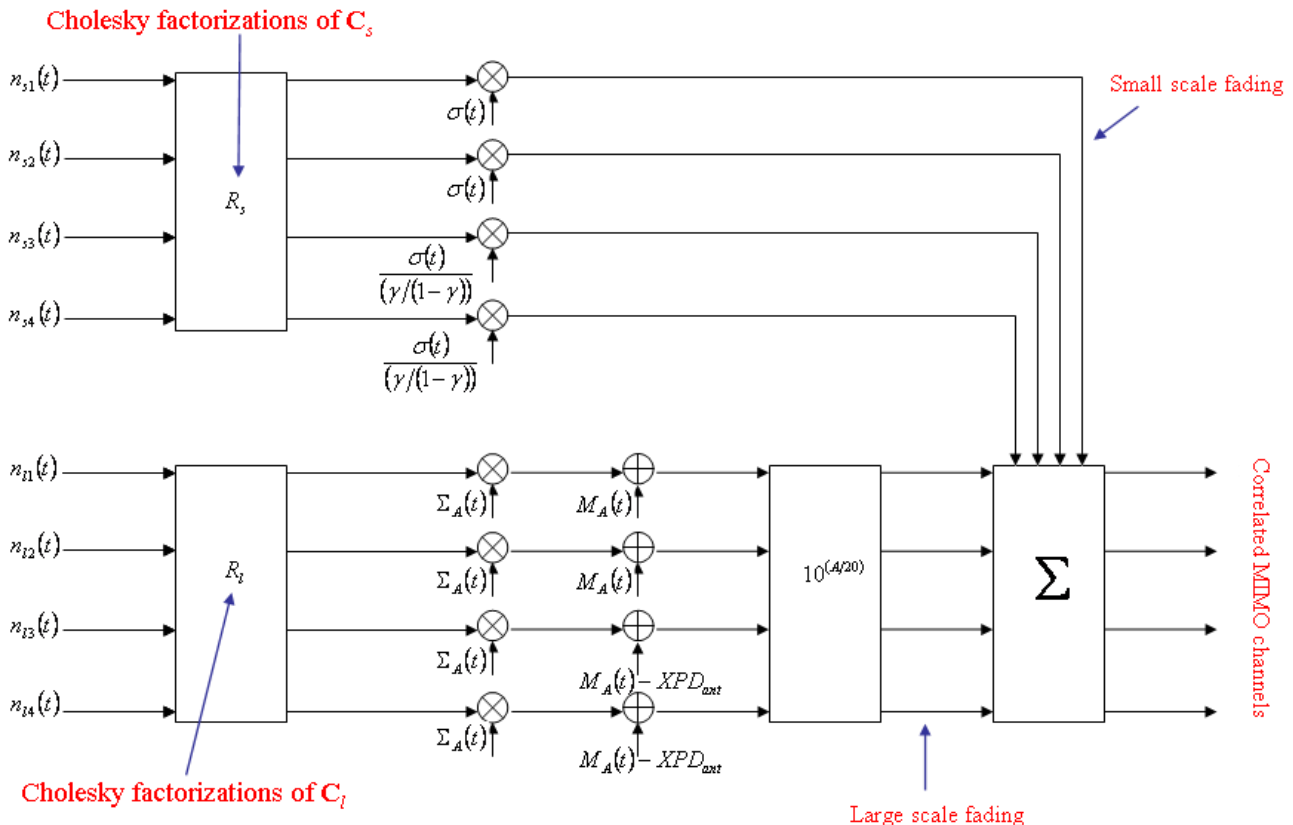


Figure 17: MIMO empirical channel model described in [16]

In [16], this analytical model is applied to the ESA 2-state Markov SISO model. The MIMO_LMS executable implements this full MIMO model. Nevertheless, applying this MIMO extension with the same

input parameters to the 3-state and the CNES 2-state models is completely possible since they fit the analytical requirements (in particular, initial processes for both large scale and small scale fadings must be normalised Gaussian processes). Moreover, this MIMO extension is already implemented in the CNES 2-state DLL. Consequently, for the Suburban and Urban environments, two alternatives exist for MIMO empirical modelling between CNES and ESA softwares. Consequently, the pros and cons detailed for SISO models (Table 15) still holds for MIMO LMS simulations.

For roadside trees environments, it is suggested to use the physical-statistical MIMO model presented in 4.3.2.2 since some information seem to be missing for this environment in the empirical approach.

4.4 SISO, MISO and SIMO systems

Appropriate transmission paths of the MIMO model may be selected to provide SISO, MISO and SIMO models.

5 REFERENCES

- [1] ETSI EN 300 744 V1.4.1 (2001-01) : Digital Video Broadcasting (DVB); Framing structure, channel coding and modulation for digital terrestrial television
- [2] TM-NGH063r5_DVB-NGH-Helsinki2_channel_models_1v5.pdf
- [3] Lacoste F., Carvalho F., Scot G., Ros B., “*Comparison of Macrocell Propagation Channels at 2.2 and 3.8 GHz*”, Conférence EuCAP, Barcelone, 2010
- [4] Lacoste F.,Carvalho F, Fontan F.P, Nunez A., Fabbro, V, Scot G., “*MISO and SIMO Measurements of the Land Mobile Satellite Propagation at S-Band*”, Conférence EuCAP, Barcelone, 2010
- [5] Y.R. Zheng, C. Xiao, “*Improved Models for the Generation of Multiple Uncorrelated Rayleigh Fading Waveforms*”, IEEE Com. letters, Vol. 6, N. 6, June 2002
- [6] M. Cheffena, F. Perez-Fontan, “*Channel simulator for land mobile satellite channel along roadside trees*”, IEEE Trans. on Ant. and Prop., Vol. 59, No. 5, May 2011.
- [7] Y. L. C. de Jong, M. H. A. J. Herben, “*A tree-scattering model for improved propagation prediction in urban microcells*”, IEEE Trans. Veh. Techn., Vol. 53, pp. 503-6513, March 2004.
- [8] T. Aulin, “*A modified model for the fading signal at a mobile radio channel*”, IEEE Trans. Veh. Technol., vol. VT-28, pp. 182–203, Aug. 1979.
- [9] M. Cheffena, F. Perez-Fontan, F. Lacoste, E. Corbel, H.-Jose Mametsan G. Carrie, “*Land Mobile Satellite Dual Polarized MIMO Channel along Roadside Trees: Modeling and Performance Evaluation*”, accepted for publication in IEEE Trans. on Ant. and Prop., 2011
- [10] P.R. King, “*Modelling and Measurement of the Land Mobile Satellite MIMO Radio Propagation Channel*”, PhD thesis, University of Surrey, UK, April 2007
- [11] Perez Fontan and all , “*S-Band LMS propagation channel behaviour for different environments, degrees of shadowing and elevation angles*”, IEEE transactions on broadcasting, Vol. 44, N°1 March 1998
- [12] Pérez-Fontán, F., Vázquez-Castro, M., Cabado, C.E., Pita García, J., Kubista, E., “*Statistical Modelling of the LMS channel*”, IEEE Transactions on Vehicular Technology, Vol. 50, No.6, Nov. 2001, pp. 1549-1567.
- [13] R. P. Cerdeira, F. Pérez Fontán, P. Burzigotti, A. Bolea Alamañac, and I. Sanchez Lago, “*Versatile two-state land mobile satellite channel model with first application to DVB-SH analysis*”, Int. J. Satell. Commun.Netw., DOI: 10.1002/sat.964, 2010.
- [14] TM-NGH 473, *MIMO_LMS executable software*, ESA, 2010
- [15] TM-NGH 472, *Reference Document for Executable “MIMO_LMS.exe” of the Dual Polarization MIMO LMS Channel Model*, ESA, 2010
- [16] K. Liolis, J. Gomez-Vilardebo, E. Casini, A. Perez-Neira, “*Statistical modeling of dual-polarized MIMO land mobile satellite channels*”, IEEE Transactions on Communications, Vol. 58, No.11, Nov. 2010, pp. 3077-3083.